# CHARACTERISTICS OF NEAR-CIRCULAR LUNAR SATELLITE ORBITS

by

DAVID HAWKINS, B.S.

THESIS

Presented to the Faculty of the Graduate School of
The University of Texas in Partial Fulfillment
of the Requirements

For the Degree of

MASTER OF SCIENCE IN AERO-SPACE ENGINEERING

THE UNIVERSITY OF TEXAS

Austin, Texas

August, 1966

This report was prepared under

NASA MANNED SPACE FLIGHT CENTER
Contract 9-2619

under the direction of

Dr. Byron D. Tapley

Associate Professor of Aerospace Engineering

and Engineering Mechanics

# PREFACE

Manned lunar missions, to be implemented under Project Apollo, will include a low altitude, near circular, lunar orbital phase of short duration. Follow-on missions may require extended time in such an orbit. Hence, pre-mission planning for operations in the near lunar space environment will be based on estimates of orbital variations for both short-and long-term motion of the space vehicle. A realistic approach to the problem of establishing orbit characteristics would necessarily include a determination of how the noncentral lunar gravitational field, acting in conjunction with the perturbing influences of the Sun and planets, will affect the vehicle's trajectory. The present investigation is concerned with this problem and was motivated, in part, by the recent acquisition of modified JPL computer tapes, providing an accurate solar system ephemeris for the years 1950 to 2000.

The author wishes to thank Dr. Byron D. Tapley, who, as supervising professor for this investigation, provided much encouragement and timely advice. The author is grateful to Dr. Wallace F. Fowler who, as a member of the supervising committee, gave many helpful suggestions concerning the computation phase of the study. The author is indebted to George H. Born who provided invaluable advice and made available the

materials and knowledge gained from his earlier investigation of lunar orbits. Finally, acknowledgment is made to Mr. C. B. Williams of The University of Texas Computation Center who assisted in resolving many of the difficulties encountered in the formulation and testing of the computer program.

David Hawkins

The University of Texas
Austin, Texas
June, 1966

# ABSTRACT

Near-circular lunar satellite orbits of low inclination, corresponding to the types planned for Apollo missions, are investigated numerically as a four-body problem. A computer program was written to numerically integrate a modified set of perturbation equations which is free of the small eccentricity restriction encountered in the classical Lagrangian set. Machine plots are obtained for the time variation of local maximum and minimum values of the short period oscillations in the orbit elements over a total time span equivalent to one complete circuit of the Moon about the Earth (the anomalistic period).

The perturbed acceleration of the satellite is generated by the second-order term of the lunar gravitational force potential and a disturbing function incorporating the effects of the Earth and Sun, both considered as point masses. The Earth-Moon node is assumed to regress at a constant rate. The computer routine receives disturbing body position data from modified JPL Ephemeris Tapes. The results for eight sets of initial conditions are presented in tabular and graphical form. It is concluded that all orbit types considered exhibit a high degree of stability for a period of 28 days.

# TABLE OF CONTENTS

Page

PREFACE . . . . . . . . . . . . . . . . . . . . . . . . iii

ABSTRACT . . . . . . . . . . . . . . . . . . . . . . . v

LIST OF FIGURES . . . . . . . . . . . . . . . . . . . . vii

LIST OF TABLES . . . . . . . . . . . . . . . . . . . . ix

NOMENCLATURE . . . . . . . . . . . . . . . . . . . . . x

CONSTANTS . . . . . . . . . . . . . . . . . . . . . . . xiii

I. INTRODUCTION . . . . . . . . . . . . . . . . . . . 1

II. ANALYSIS . . . . . . . . . . . . . . . . . . . . . 6

Problem Description and Assumptions . . . . . . 6
Modified JPL Ephemeris Tapes . . . . . . . . . 10
Coordinate Systems . . . . . . . . . . . . . . 11
Coordinate Transformations . . . . . . . . . . 13
Perturbation Equations . . . . . . . . . . . . 19
Disturbed Motion of a Lunar Satellite . . . . . 21

III. NUMERICAL COMPUTATION . . . . . . . . . . . . . 29

Computation Procedure . . . . . . . . . . . . . 29
Accuracy Estimation . . . . . . . . . . . . . . 30

IV. RESULTS . . . . . . . . . . . . . . . . . . . . . 33

Specification of Orbit Types . . . . . . . . . 33
Comparison with the Results from Reference 4 . 34
Graphical Analysis . . . . . . . . . . . . . . 37

V. CONCLUSIONS AND RECOMMENDATIONS . . . . . . . . . 54

REFERENCES . . . . . . . . . . . . . . . . . . . . . . 57

# LIST OF FIGURES

Figure Page

1 Selenocentric Coordinate Systems . . . . . . . . . 12

2 Selenocentric Orientation of Satellite Orbit . . . 22

3 Vector Representation of the Disturbed Motion of Two Bodies . . . . . . . . . . . . . . . . . . . . 23

4 Semi-Latus Rectum for Orbit Types 1 and 3. . . . . 46

5 Semi-Latus Rectum for Orbit Types 2 and 4. . . . . 46

6 Inclination for Orbit Types 1 and 2. . . . . . . . 47

7 Inclination for Orbit Types 3 and 4. . . . . . . . 47

8 Argument of Node for Orbit Types 1 and 3, P = 1822.20 KM . . . . . . . . . . . . . . . . . 48

9 Argument of Node for Orbit Types 2 and 4, P = 1981.35 KM . . . . . . . . . . . . . . . . . 48

10 Eccentricity for Orbit Types 1 and 3, P = 1822.20 KM . . . . . . . . . . . . . . . . . 49

11 Eccentricity for Orbit Types 2 and 4, P = 1981.35 KM . . . . . . . . . . . . . . . . . 49

12 Semi-Latus Rectum for Orbit Types 5 and 7. . . . . 50

13 Semi-Latus Rectum for Orbit Types 6 and 8. . . . . 50

14 Inclination for Orbit Types 5 and 6. . . . . . . . 51

15 Inclination for Orbit Types 7 and 8. . . . . . . . 51

16 Argument of Node for Orbit Types 5 and 7, P = 1822.20 KM . . . . . . . . . . . . . . . . . 52

17 Argument of Node for Orbit Types 6 and 8, P = 1981.35 KM . . . . . . . . . . . . . . . . . 52

Figure Page

18 Eccentricity for Orbit Types 5 and 7, P = 1822.20 KM . . . . . . . . . . . . . . . . . . 53

19 Eccentricity for Orbit Types 6 and 8, P = 1981.35 KM . . . . . . . . . . . . . . . . . . 53

# LIST OF TABLES

Table Page

1 End Point Data Comparison for 80 Satellite Revolutions--Prograde Orbits. . . . . . . . . . . . 35

2 End Point Data Comparison for 80 Satellite Revolutions--Retrograde Orbits. . . . . . . . . . . 36

3 Boundary Values of Orbit Elements--Prograde Orbits. 38

4 Boundary Values of Orbit Elements--Retrograde Orbits. . . . . . . . . . . . . . . . . . . . . . 39

# NOMENCLATURE

| | |
|---|---|
| $\bar{A}$ | Principal moment of inertia about $x'$ axis |
| $A$ | $e\cos\omega$ |
| $[A]$ | Coordinate transformation matrix |
| $\bar{B}$ | Principal moment of inertia about $y'$ axis |
| $B$ | $e\sin\omega$ |
| $[B]$ | Coordinate transformation matrix |
| $\bar{C}$ | Principal moment of inertia about $z'$ axis |
| $S$ | Perturbing acceleration in circumferential direction |
| $[C]$ | Coordinate transformation matrix |
| $[D]$ | Coordinate transformation matrix |
| $e$ | Eccentricity of satellite orbit |
| $f$ | True anomaly of satellite |
| $G$ | Universal gravitational constant |
| $h$ | Angular momentum of satellite |
| $H$ | Perturbing force potential |
| $I$ | Inclination of satellite orbit plane to epoch lunar equator |
| $K_1$ | Earth radius conversion factor |
| $K_2$ | Earth-Moon barycenter distance from the Moon expressed as a fraction of the total distance between the Earth and Moon |
| $K_3$ | Astronomical unit in kilometers |
| $L_m$ | Mean longitude of the Moon |

| | |
|---|---|
| $m$ | Mass of the satellite |
| $M_e$ | Mass of the Earth |
| $M_m$ | Mass of the Moon |
| $M_s$ | Mass of the Sun |
| $[M]$ | Coordinate transformation matrix |
| $P$ | Semi-latus rectum |
| $R$ | Perturbing force in radial direction |
| $R_e$ | Earth's selenocentric radius |
| $R_s$ | Sun's selenocentric radius |
| $r$ | Satellite's selenocentric radius |
| $T$ | Time in Julian centuries of 36525 days past the Epoch $0^h$ January 1, 1950, E.T.(J.D. 2433282.5) |
| $t$ | Time in seconds past J.D. 2440616.0 |
| $u$ | Angle measured from ascending node to satellite radius vector |
| $V$ | Potential energy function of Moon |
| $W$ | Perturbing acceleration normal to orbit plane |
| $x,y,z$ | Selenocentric inertial coordinates |
| $x',y',z'$ | Selenocentric body-fixed coordinates |
| $\tilde{x},\tilde{y},\tilde{z}$ | Selenocentric rotating coordinates |
| $x_e,y_e,z_e$ | Selenocentric inertial coordinates of Earth |
| $x_s,y_s,z_s$ | Selenocentric inertial coordinates of Sun |
| $\ddot{X},\ddot{Y},\ddot{Z}$ | Perturbing accelerations in x,y,z directions |
| $\overline{X}_m,\overline{Y}_m,\overline{Z}_m$ | Geocentric inertial coordinates of Moon in units of "Earth Radii" referred to the mean equinox and equator of 1950.0 |

| | |
|---|---|
| $\overline{X}_b,\overline{Y}_b,\overline{Z}_b$ | Heliocentric inertial coordinates of Earth-Moon barycenter referred to the mean equinox and equator of 1950.0 |
| $\hat{X},\hat{Y},\hat{Z}$ | Coordinates measured from axes fixed in space |
| $\alpha$ | Angle measured from $\tilde{x}$ axis to $x$ axis |
| $\delta$ | Inclination of lunar equator to ecliptic |
| $\overline{\epsilon}$ | Mean obliquity of ecliptic |
| $\theta$ | Angle measured from $\tilde{x}$ axis to $x'$ axis |
| $\theta_0$ | Value of $\theta$ for J.D. 2440616.0 |
| $\mu$ | Lunar gravitational constant |
| $\overline{\rho}_e$ | Earth's position vector from satellite |
| $\overline{\rho}_s$ | Sun's position vector from satellite |
| $\omega$ | Argument of pericentron |
| $\Omega_n$ | Longitude of the mean ascending node of the lunar orbit on the ecliptic measured from the mean equinox of date |
| $\Omega$ | Longitude of ascending node of satellite orbit measured in the epoch (J.D. 2449616.0) lunar equatorial plane from the x-axis |
| ♈ | Mean Vernal equinox of date |
| $(\overline{\ })$ | Vector notation |
| $(\dot{\ })$ | First derivative of ( ) with respect to time |
| $(\ddot{\ })$ | Second derivative of ( ) with respect to time |

# CONSTANTS

| | |
|---|---|
| $\overline{A}$ | $.88781798 \times 10^{29}$ KG-KM$^2$ |
| $\overline{B}$ | $.88800195 \times 10^{29}$ KG-KM$^2$ |
| $\overline{C}$ | $.88836978 \times 10^{29}$ KG-KM$^2$ |
| G | $.66709998 \times 10^{-19}$ KM$^3$/KG-sec$^2$ |
| $GM_e$ | $.3986032 \times 10^{6}$ KM$^3$/sec$^2$ |
| $GM_m$ | $.49027779 \times 10^{4}$ KM$^3$/sec$^2$ |
| $GM_s$ | $.132715445 \times 10^{12}$ KM$^3$/sec$^2$ |
| A.U. | $.149599000 \times 10^{9}$ KM |
| $K_1$ | $.6378327 \times 10^{4}$ KM |
| $K_2$ | 398603.2/403505.9 |
| $K_3$ | $.149599000 \times 10^{9}$ KM |
| $\overline{\epsilon}$(1950.0) | .40920619 radians |
| $\delta$ | $.1535 \times 10^{+1}$ degrees |

# I. INTRODUCTION

The potential military and political advantages associated with extensive exploration of the Moon has induced the United States and the Soviet Union to implement accelerated space programs to achieve a manned lunar landing prior to the next decade. Russia's recent successful injection of a space probe into lunar orbit demonstrates the feasibility of manned lunar missions. Current GEMINI flights of the United States are establishing effective rendezvous techniques to be used on the manned lunar missions of Project Apollo.

Apollo mission philosophy calls for injection of a manned spacecraft into near-circular lunar orbit at an altitude of from 50 to 150 miles. A lunar excursion vehicle will separate from the command module, descend to a preselected point above the Moon's surface, and make a soft landing. After a suitable lunar stay, the excursion vehicle will be launched from the lunar surface and will rendezvous with the orbiting stage. Successful execution of this near-lunar phase will depend on an accurate determination of the orbiting stage position and the capability of predicting its motion. It is, therefore, essential that the characteristics of lunar satellite orbits be established prior to mission execution.

In contrast with the well documented Earth-satellite problem, relatively little has been published on the equivalent lunar problem. Because of the lack of similarity between Earth and Moon satellite theory, little new information on the lunar problem can be gained by comparing the two types. An introduction to lunar satellite theory is presented in Reference 17.[*] A comprehensive discussion of the basic geometry of the Earth-Moon system appears in Reference 3. The details associated with the development of the perturbation theory used in this report may be found in References 9, 19 and 20.

Some of the published investigations to date reveal two quite different approaches to the lunar satellite problem. One approach leads to approximate closed form solutions to Lagrange's Planetary equations, a set of first-order nonlinear differential equations for the time variation of the orbit elements. Another method employs high speed digital computation to numerically integrate the perturbation equations. In general, the first approach is suited to studies of long term motion, while the numerical approach is usually limited to studies of short term motion from a consideration of economy with respect to machine computation time.

Lass and Solloway[15] obtain approximate solutions for the motion of a satellite of the Moon by simplifying Lagrange's equations and by using the averaging process of Kryloff-Bogolinboff. Solar effects are neglected and the Moon is assumed to be a triaxial ellipsoid in circular orbit about a point mass Earth. They conclude that a lunar satellite initially in a circular polar orbit of small radius will deviate little from this configuration over a period of six months. Lorell,[17] using the same Earth-Moon model, estimates the relative importance of lunar, Earth and solar gravitational effects on a satellite based on some long term and secular variations of the orbit elements. Tolson[24] has developed a first-order approximation to the equations of satellite motion neglecting all perturbing effects except the Moon's noncentral force field. From a first-order solution to the perturbation equations, Wells[25] determines the effect of the Moon's third zonal harmonic on the satellite's pericenter distance. He obtains an envelope for initial orbit orientation that will result in long satellite lifetimes, where "lifetime" means the time associated with a 36-kilometer change in pericenter distance.

---

[*] References appear on pp. 57-58.

Numerical integration of Lagrange's equations, or alternately the equations of motion, has been reported by several investigators, three of which are mentioned here. Brumberg[6] assumes a point mass Earth and Sun and uses two body equations to describe their motion with respect to the Moon, which is considered a triaxial ellipsoid. The satellite equations of motion are integrated over a period of 40 revolutions for both polar and equatorial orbits of large and small eccentricities. A tabulation of initial and final orbit element values shows all orbits to be highly stable. It is interesting to note, in view of the Lass and Solloway conclusion, that the small eccentricity polar orbit shows practically no deviation from the initial orbit orientation. A similar study has been reported by Goddard[11] who obtains a computer solution to Lagrange's equations for the same orbit types considered by Brumberg. Goddard, however, excludes the Sun and considers a point mass Earth in circular orbit about the Moon. A comparison of end point values of the orbit elements, for two polar orbits, with those obtained by Brumberg reveals a significant disagreement, especially for the semimajor axis. The fact that these investigators used different numerical integration methods (each having a different accuracy standard) and significantly different mesh sizes could account for the disagreement.

Goddard's computer program has since been modified by Born[4] who assumes a point mass Earth moving in a Keplerian ellipse about the Moon. Initial orientation of the Earth-Moon system is determined from a truncated form of Brown's series expansions given in Reference 2. By retaining only local maximum and minimum orbit element values of the short period variations, Born obtains an envelope for these variations for 80 revolutions of the satellite (equivalent to about 7 mean solar days). He considers circular orbits at two altitudes, 50 and 150 miles from the lunar surface, having inclinations of 0.5°, 10° and 20° (direct orbits) and 160°, 170° and 179.5° (retrograde orbits). He concludes that all orbit types exhibit a high degree of stability for a period of 80 revolutions, and that there is no indication of future instability. Born recommends that the integrations be carried out over a period of one month and that the study be expanded to include solar effects. Based on anticipated perturbations of lunar orbiters, Kaula[14] suggests that determination of the amplitudes of semi-monthly and monthly oscillations of the orbit elements would be desirable.

The investigation described herein was motivated by the foregoing recommendations and the recent acquisition of JPL Ephemeris Tapes, modified for use with the CDC 1604 computer at The University of Texas. The tapes contain position and velocity coordinates, accurate to 12 decimal digits, of the major bodies of the solar system. A completely new computer program was written, incorporating the integration method (Adams-Moulton) used by Born, to include solar effects, to provide for a regressing Earth-Moon node, and to provide the capability of obtaining Earth and Sun position data from the Ephemeris Tapes. A modified set of Lagrange's Planetary (perturbation) equations, defining the time variation of the satellite orbit elements, are numerically integrated over an interval of 27.55 days. Initial conditions are identical to those of Born, except that inclinations of 10° and 170° are not considered. In the Results Section initial and final values of the orbit elements are tabulated, and envelopes of the short period variations are presented graphically. Presented also, is a tabular comparison with Born's results, based on 80 revolutions.

# II. ANALYSIS

## A. Problem Description and Assumptions

Due to the rather complex nature of the lunar satellite problem, realistic solutions are usually not easy to obtain. The degree of problem complexity will depend mainly on desired accuracy limits. The simple, closed-form, two-body solution is obtained with ease, but it is hopelessly inadequate for describing the true motion of a lunar satellite. The presence of other celestial bodies, such as the Earth and Sun, will cause the satellite to deviate from an elliptical path, so that the orbit elements will vary with time. A reasonably accurate account of the motion requires consideration of the highly nonlinear n-body problem, for which no closed-form solution exists. Fortunately, the digital computer provides a means for attacking the problem in its most general form. On the other hand, computer limitations and lack of precision in the physical constants make it desirable to simplify the problem to the extent possible without compromising desired accuracy limits. For this analysis the limits are arbitrarily set at ± 100 meters in satellite range. This error tolerance is equivalent to precision through five decimal digits for the orbit types considered.

The perturbing forces that will influence the motion of the satellite are caused by the following:

(1) Moon's noncentral gravity field

(2) Earth's gravity field

(3) Sun's gravity field

(4) Gravity fields of the planets

(5) Gravity fields of bodies exterior to the solar system

(6) Solar radiation pressure.

The relative importance of these perturbing factors depends on the type of satellite and its orbit geometry. According to Lass and Solloway,[15] the principal perturbing affects on a near-lunar satellite are caused by the first three effects in the above list. They estimate that the Moon's perturbing effect on a satellite is slightly more dominant than the Earth's effect, the latter being about 200 times greater than the Sun's effect. The relative importance of planetary influences can be estimated by applying Newton's inverse square law of gravitation ($F/m = GM_i/r^2$), where $F/m$ is the acceleration of a satellite of mass $m$ and $M_i$ is the mass of the disturbing body at a distance $r$ from the satellite. Calculations for each planet at inferior conjunction will yield the maximum acceleration. It is found that the Sun produces a satellite acceleration of approximately $6 \times 10^{-6}$ KM/sec$^2$ and that planetary effects range from $3 \times 10^{-10}$ KM/sec$^2$ for Jupiter to $1 \times 10^{-14}$ KM/sec$^2$ for Pluto. The nearest star, Alpha Centuri, at a distance of 4.3 light years from the Sun, will have an effect of the order to $10^{-15}$ KM/sec$^2$. Here, the star is assumed to be as massive as the Sun. For a satellite of high density, it can be shown that the solar radiation effect is smaller than Jupiter's effect. Since Jupiter's effect is extremely small compared to the Sun's effect, the initial decision was to temporarily neglect all perturbing forces except those due to the Moon, Earth and Sun, pending computer test runs to determine the importance of solar effects. Subsequently, two computer runs were made, one including the Sun and the other neglecting it. Comparison of the two sets of results showed that the amplitude of the oscillations of the semi-latus rectum was changed by about 0.05%, which is equivalent to a change in satellite position of less than one meter. The other orbit elements showed changes that were less than 0.05%. The results of this test confirms the soundness of the original decision. Moreover, the Earth and Sun can be treated as point masses, because the effect of their noncentral gravity fields on a near-lunar satellite is negligible for studies of short-term motion. The lunar noncentral gravity field, however, will have significant effects on a satellite that is close to the Moon.

It is generally conceded that a triaxial ellipsoid closely approximates the true shape of the Moon. Since very little is known concerning the Moon's mass distribution, it has been common practice to assume that it is uniform throughout. It will be necessary, later in this analysis, to relate the inertial coordinates of the satellite to the principal axes of inertia of the Moon. To achieve a high degree of accuracy, this particular transformation must account for the mean rate of regression of the ascending node of the Earth-Moon orbit (about

1.5° per month), the nodes libration in longitude, and the Moon's dynamic librations in latitude and longitude. According to Kalensher,[13] the maximum monthly variation of these librations is less than 0.005°, which is quite small relative to the mean rate of change of the node.

In view of what has been said in the foregoing discussion, the mathematical formulations for this analysis are based on the following assumptions:

(1) The only significant perturbing influences are due to the Moon's noncentral gravity field and the gravity fields of the Earth and Sun.

(2) The Earth and Sun are point masses.

(3) The mass of the satellite is negligible compared to the Moon's mass.

(4) The Moon is a triaxial ellipsoid of uniform mass distribution.

(5) Neglecting the libration of the mean ascending node of the Earth-Moon orbit and the dynamic librations of the Moon in latitude and longitude will have a negligible effect on the accuracy of the results.

These assumptions must be incorporated into a set of perturbation equations which define the time rates of change of the satellite orbit elements. Before introducing these equations, it will be instructive to describe the Modified JPL Ephemeris Tapes, and to define coordinate systems and pertinent transformations.

## B. Modified JPL Ephemeris Tapes

The Jet Propulsion Laboratory of the California Institute of Technology has developed an ephemeris for the major bodies of the solar system. Position and velocity data, accurate to 12 places, has been stored on magnetic computer tapes to be used with the IBM 7090 computer in conjunction with the JPL Space Trajectories Program.[12]

JPL tapes, covering the years 1950-2000, have been recently modified for use with the Control Data Corporation 1604 computer at The University of Texas. A description of the modified tapes and directions for their use may be found in Reference 7. Tape data required for this study consists of the heliocentric coordinates, in astronomical units, of the Earth-Moon barycenter and the geocentric coordinates of the Moon in units of Earth radii. The position and velocity components are referred to a rectangular cartesian coordinate system whose reference plane and reference direction coincide with the mean equator and equinox of 1950.0 (Julian Date 2433282.423357). The standard constants for converting astronomical units and Earth radii to kilometers, as given in Reference 8, are 1 A.U. = 149599000KM and 1 Earth radius = 6378.3255 KM. However, the value of one Earth radius used for this investigation, and the value recommended according to Reference 22, is 1 Earth radius = 6378.327 KM. The difference in these two values (0.0015 KM) results in an insignificant difference (less than 0.09 KM) in the Earth's selenocentric coordinates. Hence, for this study, either value of this conversion constant could be used.

## C. Coordinate Systems

For this analysis three selenocentric coordinate systems are specified in addition to the 1950.0 system associated with the JPL Ephemeris Tape data. All coordinate systems are orthogonal and right-handed in the vector sense.

(1) Selenocentric "Inertia" System (x,y,z). For convenience in referencing the satellite orbit elements, the primary coordinate system is chosen such that its origin is at the Moon's center of mass and its angular orientation is invariant with respect to a fixed direction. This system is not "inertial" in the absolute sense, because the origin is translating along a curved path relative to the Sun. However, by virtue of the nonrotating feature, the equations of relative motion, based on Newton's law, are valid. At time zero for this study the x-axis is defined by the intersection of the lunar equatorial plane and the ecliptic plane, and it is directed towards the mean ascending node of the Earth-Moon orbit (see Fig. 1). If the z-axis coincides with the Moon's spin axis and if it is directed towards the north celestial hemisphere, the y-axis will lie in the lunar equatorial plane.

(2) Body-Fixed Selenocentric System (x',y',z'). The (x',y',z')-coordinate system shown in Fig. 1 will coincide with the Moon's principal axes of inertia such that the x'-axis is directed toward the Earth and the z'-axis is directed towards the north celestial hemisphere. Since this system is body-fixed, it will rotate with the Moon and the z'-axis will always be coincident with the Moon's spin axis.

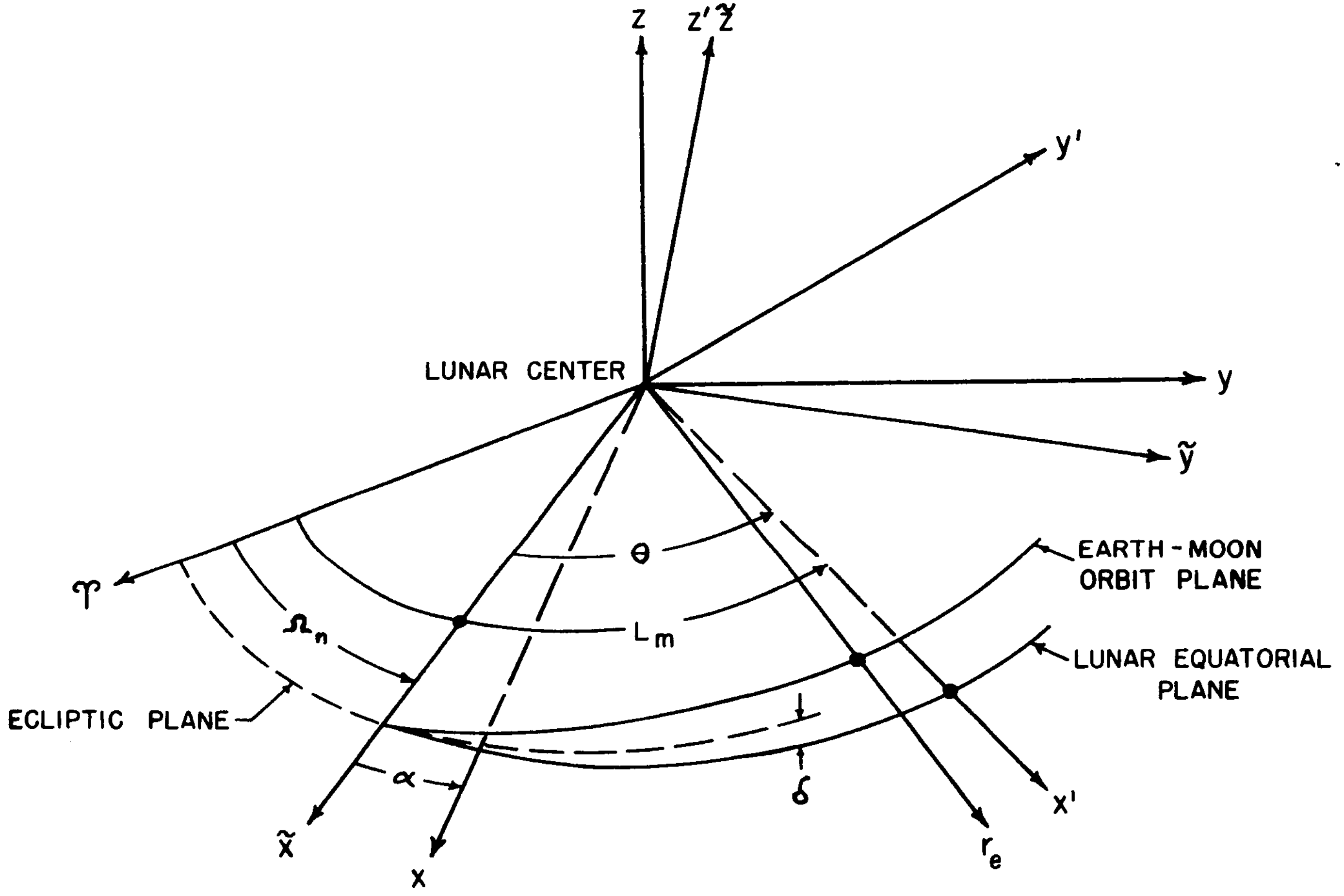
Z
Z' $\tilde{Z}$
y'
LUNAR CENTER
y
$\tilde{y}$
$\theta$
$L_m$
$\Omega_n$
♈
EARTH - MOON ORBIT PLANE
LUNAR EQUATORIAL PLANE
ECLIPTIC PLANE
$\delta$
$\alpha$
$\tilde{x}$
x
$r_e$
x'

FIGURE 1. SELENOCENTRIC COORDINATE SYSTEMS.

(3) Rotating Selenocentric System $(\tilde{x},\tilde{y},\tilde{z})$. To relate the regressional motion of the line of nodes of the Earth-Moon system to the primary coordinate system, define the Moon centered $(\tilde{x},\tilde{y},\tilde{z})$-system such that the $\tilde{x}$-axis is in the ecliptic plane and is always directed towards the mean ascending node of the Earth-Moon orbit as shown in Fig. 1. At time zero the $(\tilde{x},\tilde{y},\tilde{z})$-coordinate system will be coincident with the $(x,y,z)$-system. The rotational motion of the $(\tilde{x},\tilde{y},\tilde{z})$-coordinates (viewed from the positive $\tilde{z}$-axis) will be described by a clockwise rotation about a line which is normal to the ecliptic plane.

(4) Reference for Solar System Ephemerides $(\overline{X},\overline{Y},\overline{Z})$. It will be seen later that the equations for the perturbing acceleration of a lunar satellite will contain the coordinates of the Earth and Sun referred to the primary system. As was mentioned previously, the modified JPL Ephemeris Tapes provide heliocentric Earth-Moon barycenter position (in A.U.) and geocentric lunar position (in Earth radii) referred to the system of the mean equinox and equator of 1950.0. To distinguish between the two different origins, let $\overline{X}_b,\overline{Y}_b,\overline{Z}_b$ denote heliocentric barycenter coordinates and $\overline{X}_m,\overline{Y}_m,\overline{Z}_m$ denote geocentric lunar coordinates.

## D. Coordinate Transformations

Three different coordinate transformations are required for the subsequent computations. The first two relate Earth and Sun coordinates in the 1950.0 system to the selenocentric inertial system. The third relates satellite inertial coordinates to the selenocentric body-fixed system (x',y',z').

(1) Transformations for Earth and Sun Coordinates. The selenocentric inertial coordinates of the Earth and Sun are given by

$$\begin{bmatrix} x_e \\ y_e \\ z_e \end{bmatrix} = -K_1[D][C][B][A]\begin{bmatrix} \overline{X}_m \\ \overline{Y}_m \\ \overline{Z}_m \end{bmatrix} \tag{1}$$

$$\begin{bmatrix} x_s \\ y_s \\ z_s \end{bmatrix} = K_2\begin{bmatrix} x_e \\ y_e \\ z_e \end{bmatrix} - K_3[D][C][B][A]\begin{bmatrix} \overline{X}_b \\ \overline{Y}_b \\ \overline{Z}_b \end{bmatrix} \tag{2}$$

where the e and s subscripts denote the Earth and Sun, respectively. The quantities $K_1$, $K_2$, $K_3$ are conversion constants and [A], [B], [C], [D] are rotation matrices to be shown in detail later in this section. The recommended value for $K_1$ (Reference 22) and the standard values for $K_2$ and $K_3$ (Reference 7) are

$$K_1 = 6378.327$$

$$K_2 = 398603.2/403505.9$$

$$K_3 = 149599000.0$$

where $K_1$ is the number of kilometers in one Earth radius, $K_2$ is the Earth-Moon barycenter distance from the Moon expressed as a fraction of the total distance between the Earth and the

Moon, and $K_3$ is the number of kilometers in one astronomical unit. Matrix A transforms coordinates referred to the mean equinox and equator of 1950.0 to coordinates referred to the mean equinox and equator of date. It is given by the following expression[12]

$$A = \begin{bmatrix} a_{11} & a_{12} & a_{13} \\ a_{21} & a_{22} & a_{23} \\ a_{31} & a_{32} & a_{33} \end{bmatrix} .$$

The matrix elements are defined by

$a_{11} = 1 - 0.00029697\ T^2 - 0.00000013\ T^3$

$a_{12} = - a_{21} = - 0.02234988\ T - 0.00000676\ T^2 + 0.00000221\ T^3$

$a_{13} = - a_{31} = - 0.00971711\ T + 0.00000207\ T^2 + 0.00000096\ T^3$

$a_{22} = 1 - 0.00024976\ T^2 - 0.00000015\ T^3$

$a_{23} = a_{32} = - 0.00010859\ T^2 - 0.00000003\ T^3$

$a_{33} = 1 - 0.00004721\ T^2 + 0.00000002\ T^3$

where $T$ is the number of Julian centuries of 36525 days past the epoch $0^h$ January 1, 1950, E.T. (J.D. 2433282.5), hereafter referred to as the "Epoch." Note that the expression for $a_{11}$ is listed incorrectly in Reference 7. Matrix B rotates coordinates referenced to the mean equinox and equator of date through the angle $\bar{\epsilon}$, where $\bar{\epsilon}$ is the mean obliquity of date. It is defined by the following

$$B = \begin{bmatrix} 1 & 0 & 0 \\ 0 & \cos\bar{\epsilon} & \sin\bar{\epsilon} \\ 0 & -\sin\bar{\epsilon} & \cos\bar{\epsilon} \end{bmatrix} .$$

A truncated expression for $\overline{\epsilon}$, as given in Reference 13, is

$$\overline{\epsilon} = 23.^\circ4457874 - 0.^\circ01301376\ T - 0.^\circ8855 \times 10^{-6}\ T^2 + 0.^\circ503 \times 10^{-6}\ T^3$$

where T is defined as before. Matrix C transforms ecliptic coordinates, referenced to the mean equinox of date, to ecliptic coordinates referenced to the selenocentric inertial x-axis and is defined by

$$C = \begin{bmatrix} \cos \Omega_n & \sin \Omega_n & 0 \\ -\sin \Omega_n & \cos \Omega_n & 0 \\ 0 & 0 & 1 \end{bmatrix}$$

where $\Omega_n$ is the longitude of the mean ascending node of the lunar orbit on the ecliptic, measured from the mean equinox of date, and is given by[12]

$$\Omega_n = 12.^\circ1127902 - 0.^\circ0529539222\ d + 20.^\circ795 \times 10^{-4}\ T + 20.^\circ81 \times 10^{-4}\ T^2 + 0.^\circ02 \times 10^{-4}\ T^3$$

where T is defined as before and d is the number of ephemeris days elapsed since the "Epoch." Matrix D rotates the coordinates obtained from the previous transformation through the angle $\delta$, about the x-axis. Hence,

$$D = \begin{bmatrix} 1 & 0 & 0 \\ 0 & \cos \delta & -\sin \delta \\ 0 & \sin \delta & \cos \delta \end{bmatrix}$$

where $\delta$ is the inclination of the mean lunar equator to the ecliptic and is assigned the constant value of 1.°535, as listed in Reference 1.

(2) Satellite Coordinate Transformation. The satellite selenocentric inertial coordinates are transformed to selenocentric body-fixed (x',y',z')-coordinates by the following formulas

$$\begin{bmatrix} x' \\ y' \\ z' \end{bmatrix} = \begin{bmatrix} \cos\theta & \sin\theta & 0 \\ -\sin\theta & \cos\theta & 0 \\ 0 & 0 & 1 \end{bmatrix} \begin{bmatrix} \tilde{x} \\ \tilde{y} \\ \tilde{z} \end{bmatrix}$$

$$\begin{bmatrix} \tilde{x} \\ \tilde{y} \\ \tilde{z} \end{bmatrix} = \begin{bmatrix} 1 & 0 & 0 \\ 0 & \cos\delta & -\sin\delta \\ 0 & \sin\delta & \cos\delta \end{bmatrix} \begin{bmatrix} \cos\alpha & -\sin\alpha & 0 \\ \sin\alpha & \cos\alpha & 0 \\ 0 & 0 & 1 \end{bmatrix} \begin{bmatrix} 1 & 0 & 0 \\ 0 & \cos\delta & \sin\delta \\ 0 & -\sin\delta & \cos\delta \end{bmatrix} \begin{bmatrix} x \\ y \\ z \end{bmatrix}$$

The quantities $\theta$, $\alpha$ and $\delta$ are shown in Fig. 1. The angle $\theta$ is measured in the lunar equatorial plane between the $\tilde{x}$-axis and the x'-axis. The angle $\alpha$ is measured in the ecliptic plane between the $\tilde{x}$-axis and the x-axis. Since the libration in longitude of the Earth-Moon node and the Moon's dynamical librations are neglected in this analysis, the following expressions can be used

$$\theta = \theta_0 + \dot{\theta}t$$

$$\theta_0 = (L_m - \Omega_n - 180°)_0$$

$$\dot{\theta} = \dot{L}_m - \dot{\Omega}_n$$

$$\alpha = -\dot{\Omega}_n t$$

where $\theta_0$ is the value of $\theta$ evaluated at J.D. 2440616.0, t is the number of seconds past this epoch, $L_m$ is the mean longitude of the Moon measured in the ecliptic from the mean equinox of date to the mean ascending node of the lunar orbit, and then along the lunar equator. The dots denote derivatives with respect to time. Expressions for the remaining quantities are given in Reference 12 as

$$L_m = 64^\circ\!.37545167 + 13^\circ\!.1763965268\ d - 11^\circ\!.31575 \times 10^{-4}\ T - 11^\circ\!.3015 \times 10^{-4}\ T^2 + 0^\circ\!.019 \times 10^{-4}\ T^3$$

$$\dot{L}_m = 0.266170762 \times 10^{-5} - 0.12499171 \times 10^{-13}\ T \quad \text{rad/sec}$$

$$\dot{\Omega}_n = -\ 0.1069698435 \times 10^{-7} + 0.23015329 \times 10^{-13}\ T \quad \text{rad/sec.}$$

The term linear in T in the equations for $\dot{L}_m$ and $\dot{\Omega}_n$ can be neglected since, for the time period of interest (T = 0.2), its value is negligible compared to the value of the constant term. Then, at time zero (J.D. 2440616.0), we have

$$\theta = 0.8674880674 + 0.26724046044(10^{-5})t$$

$$\alpha = 0.1069698435(10^{-7})t$$

where $\theta$ and $\alpha$ are expressed in radians. Combining the coordinate rotation matrices yields the following expression

$$\begin{bmatrix} x' \\ y' \\ z' \end{bmatrix} = \begin{bmatrix} m_{11} & m_{12} & m_{13} \\ m_{21} & m_{22} & m_{23} \\ m_{31} & m_{32} & m_{33} \end{bmatrix} \begin{bmatrix} x \\ y \\ z \end{bmatrix} \tag{3}$$

where

$$m_{11} = \cos\theta \cos\alpha + \sin\theta \sin\alpha \cos\delta$$

$$m_{21} = -\sin\theta \cos\alpha + \cos\theta \sin\alpha \cos\delta$$

$$m_{31} = \sin\alpha \sin\delta$$

$$m_{12} = - \cos\theta \sin\alpha \cos\delta + \sin\theta\ (\cos\alpha \cos^2\delta + \sin^2\delta)$$

$$m_{22} = \sin\theta \sin\alpha \cos\delta + \cos\theta(\cos\alpha \cos^2\delta + \sin^2\delta)$$

$$m_{32} = - \sin\delta \cos\delta(1 - \cos\alpha)$$

$$m_{13} = - \cos\theta \sin\alpha \sin\delta - \sin\theta \sin\delta \cos\delta(1 - \cos\alpha)$$

$$m_{23} = \sin\theta \sin\alpha \sin\delta - \cos\theta \sin\delta \cos\delta(1 - \cos\alpha)$$

$$m_{33} = \cos\alpha \sin^2\delta + \cos^2\delta$$

## E. Perturbation Equations

In general, six parameters, or orbit elements, will describe a satellite orbit. For Keplerian two-body motion the elements are constant. When other bodies are present or when the primary body is asymmetrical, the simple two-body orbit is perturbed such that the orbit elements show a variation with time. A classical set of perturbation equations (due to Lagrange), which give the time variation of the orbit elements, are developed in Reference 19. Since these equations contain singularities for zero eccentricity, they are not used in problems involving circular orbits. An alternate set of equations, which do not possess the zero eccentricity restriction, are derived in Reference 4. These equations are adopted for this investigation. They are given by the following expressions:

$$\dot{P} = \frac{2hr}{\mu}(S)$$

$$\dot{I} = \frac{r}{h}\cos u(W)$$

$$\dot{\Omega} = \frac{r}{h}\frac{\sin u}{\sin I}(W) \qquad \text{(cont.)}$$

$$\dot{A} = B\,\dot{\Omega}\cos I + \frac{r}{h}\left\{\psi \sin u(R) + [A + (1 + \psi)\cos u](S)\right\}$$

$$\dot{B} = -A\,\dot{\Omega}\cos I + \frac{r}{h}\left\{-\psi \cos u(R) + [B + (1 + \psi)\sin u](S)\right\}$$

$$\dot{u} = \frac{h}{r^2} - \dot{\Omega}\cos I \qquad (4)$$

where the following definitions apply:

$P$ : Semi-latus rectum

$I$ : Inclination of the satellite orbit plane to the lunar equatorial plane

$\Omega$ : Longitude of ascending node

$A$ : Eccentricity times the cosine of the argument of pericenter ($e \cos \omega$)

$B$ : Eccentricity times the sine of the argument of pericenter ($e \sin \omega$)

$u$ : Argument of pericenter plus the true anomaly ($\omega + f$)

$\psi$ : $1 + A \cos u + B \sin u$

$R$ : Component of the perturbing force in the direction of the satellite radius vector

$S$ : Component of the perturbing force perpendicular to the satellite radius vector and in the orbit plane

$W$ : Component of the perturbing force normal to the orbit plane

$h$ : Satellite angular momentum

$r$ : Selenocentric radius of satellite

$\mu$ : Lunar gravitational constant.

The dots in Eqs. (4) denote derivatives with respect to time. Since these equations have a singularity at zero inclination, equatorial orbits are prohibited. The selenocentric orientation of the satellite orbit plane is shown in Fig. 2.

## F. Disturbed Motion of a Lunar Satellite

As indicated earlier, an exact description of the perturbed motion of a lunar satellite requires a solution to the n-body problem. However, it was pointed out that for practical purposes the problem may be reduced to one involving the satellite, Moon, Earth and Sun. The equations which govern the satellite's motion relative to the selenocentric inertial reference frame will now be developed. Let the $(\hat{X},\hat{Y},\hat{Z})$-coordinate system be fixed in space such that the axes are parallel to the corresponding selenocentric nonrotating $(x,y,z)$-axes. Let $M_m$ denote the Moon's mass, $m$ the satellite's mass, and $M_i$ the mass of the ith disturbing body. The position vectors for the respective bodies are defined in Fig. 3. Then, the equations of absolute motion of the Moon and the satellite are

$$M_m \ddot{\bar{r}}_1 = \frac{GM_m m}{r_{12}^3}(\bar{r}_2 - \bar{r}_1) + \sum_{i=3}^{4} \frac{GM_m M_i}{r_{1i}^3}(\bar{r}_i - \bar{r}_1) \tag{5}$$

$$m\ddot{\bar{r}}_2 = \frac{GM_m m}{r_{21}^3}(\bar{r}_1 - \bar{r}_2) + \sum_{i=3}^{4} \frac{GM_i m}{r_{2i}^3}(\bar{r}_i - \bar{r}_2) \quad . \tag{6}$$

Now, on subtracting Eq. (5) from Eq. (6) and noting that

$$\bar{r} = \bar{r}_2 - \bar{r}_1 \quad , \quad \dot{\bar{r}} = \dot{\bar{r}}_2 - \dot{\bar{r}}_1 \quad , \quad \ddot{\bar{r}} = \ddot{\bar{r}}_2 - \ddot{\bar{r}}_1$$

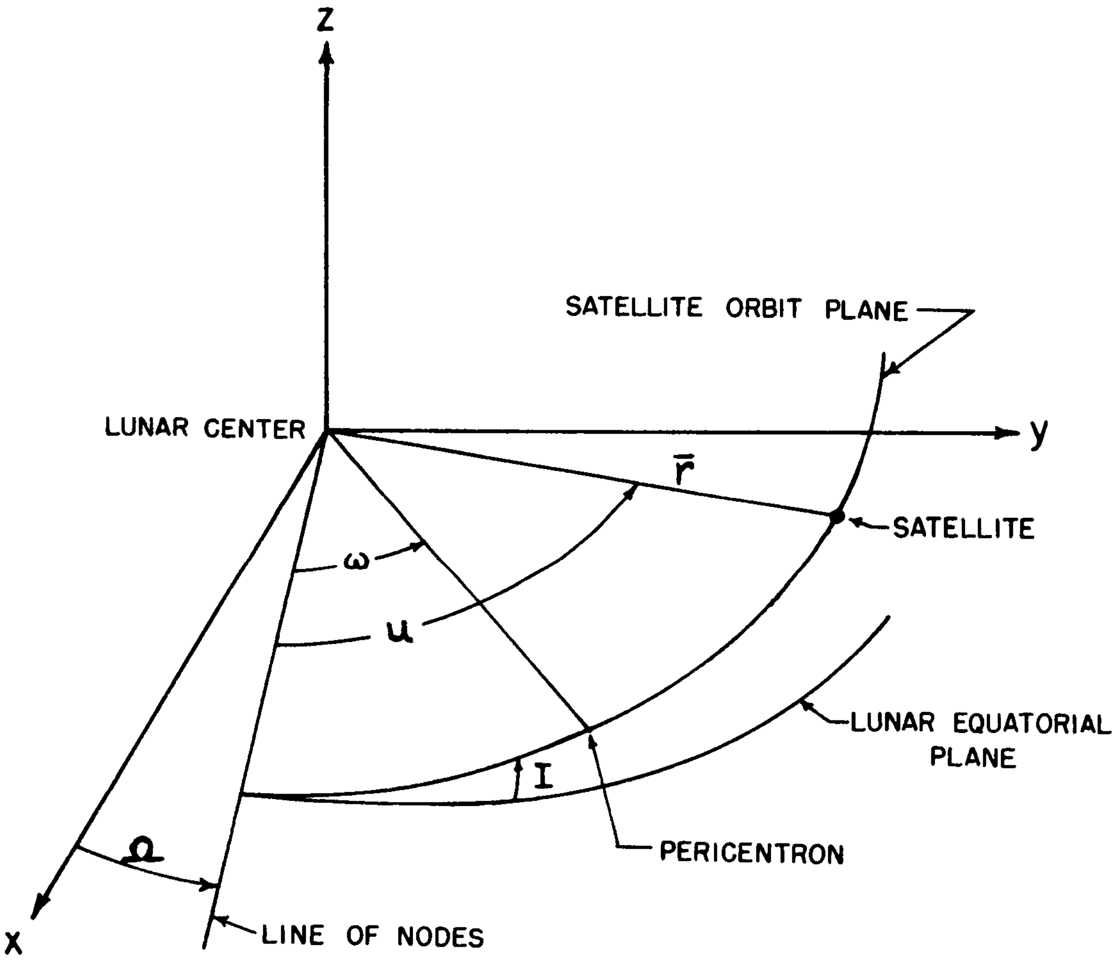
Z
SATELLITE ORBIT PLANE
LUNAR CENTER
y
$\bar{r}$
SATELLITE
ω
u
LUNAR EQUATORIAL PLANE
I
Ω
PERICENTRON
X
LINE OF NODES

FIGURE 2. SELENOCENTRIC ORIENTATION OF SATELLITE ORBIT.

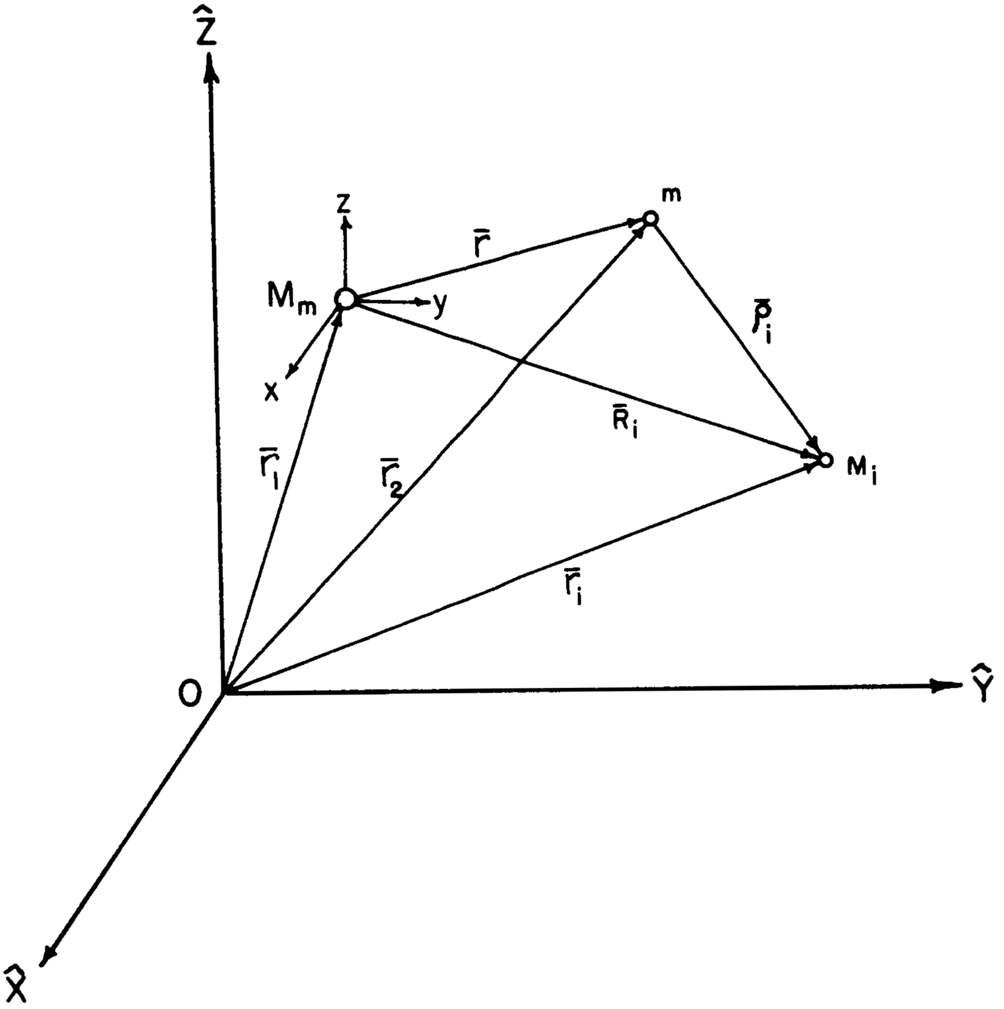
$\hat{Z}$
z
m
$\bar{r}$
$M_m$
y
x
$\bar{\rho}_i$
$\bar{R}_i$
$\bar{r}_1$
$\bar{r}_2$
$M_i$
$\bar{r}_i$
O
$\hat{Y}$
$\hat{X}$

FIGURE 3. VECTOR REPRESENTATION OF THE DISTURBED MOTION OF TWO BODIES.

the following equation is obtained

$$\ddot{\bar{r}} = -\frac{\mu\bar{r}}{r^3} + \sum_{i=3}^{4} GM_i\left[\frac{\bar{\rho}_i}{\rho_i^3} - \frac{\bar{R}_i}{R_i^3}\right] \tag{7}$$

where $\mu = G(M_m + m)$. Equation 7 defines the satellite's acceleration relative to a primary body that is spherical in shape and has a uniform mass distribution. A satellite in close orbit of the Moon will, however, be materially affected by a noncentral force field caused by an asymmetrical distribution of the lunar mass. To account for the Moon's noncentral force effects, the equation of motion is modified by replacing the central force term with the gradient of the lunar potential function. Hence, Eq. (7) may be written in expanded form as

$$\ddot{\bar{r}} = -\bar{\nabla}V - GM_e\left[\frac{\bar{R}_e}{R_e^3} - \frac{\bar{\rho}_e}{\rho_e^3}\right] - GM_s\left[\frac{\bar{R}_s}{R_s^3} - \frac{\bar{\rho}_s}{\rho_s^3}\right]$$

where $V$ represents the Moon's gravitational potential function and

$$\bar{\nabla} = \frac{\partial}{\partial x}\bar{i} + \frac{\partial}{\partial y}\bar{j} + \frac{\partial}{\partial z}\bar{k} \quad .$$

The $e$ and $s$ subscripts refer to the Earth and Sun, respectively. Now, the potential function ($V$) may be expressed in the form

$$V = \sum_{i=1}^{\infty} V_i$$

where the terms $(V_i)$ in this expansion are given through the fourth order in Reference 5 (pp. 121-128). For a triaxial ellipsoid of uniform mass distribution, and for a coordinate system chosen so that the origin is at the center of mass, it can be shown that the odd orders of V are zero. If even orders greater than two are neglected, then an approximation for the potential function is given by the expression

$$V = -\frac{GM_m}{r} - \frac{G}{2}\left[\frac{\bar{A}+\bar{B}+\bar{C}}{r^3} - 3\,\frac{\bar{A}\left(\frac{x'}{r}\right)^2 + \bar{B}\left(\frac{y'}{r}\right)^2 + \bar{C}\left(\frac{z'}{r}\right)^2}{r^3}\right]$$

where $\bar{A}$, $\bar{B}$ and $\bar{C}$ are the principal moments of inertia of the Moon. The satellite distance is given by

$$r^2 = x^2 + y^2 + z^2 = (x')^2 + (y')^2 + (z')^2 \quad .$$

The x-component of the gravitational force is determined from the partial differentiation

$$\bar{\nabla}_x V = \frac{\partial V}{\partial r}\frac{\partial r}{\partial x} + \frac{\partial V}{\partial x'}\frac{\partial x'}{\partial x} + \frac{\partial V}{\partial y'}\frac{\partial y'}{\partial x} + \frac{\partial V}{\partial z'}\frac{\partial z'}{\partial x} \quad .$$

In view of the above definition for V, this leads to the following expression

$$\bar{\nabla}_x V = \frac{GM_m}{r^2} - G\left\{\left[-\frac{3}{2}\,\frac{\bar{A}+\bar{B}+\bar{C}}{r^4} + \frac{15}{2}\,\frac{\bar{A}\left(\frac{x'}{r}\right)^2 + \bar{B}\left(\frac{y'}{r}\right)^2 + \bar{C}\left(\frac{z'}{r}\right)^2}{r^4}\right]\frac{x}{r} - \frac{3}{r^5}\left[\bar{A}m_{11}x' + \bar{B}m_{21}y' + \bar{C}m_{31}z'\right]\right\}$$

Similar expressions may be obtained for the y and z force components. Since the forces of interest are those that cause perturbations in central force field motion, the term $GM_m/r^2$ is removed in the process of defining the components of the perturbing acceleration. Then, if we define

$$H = -\frac{3}{2}\,\frac{\bar{A} + \bar{B} + \bar{C}}{r^4} + \frac{15}{2}\,\frac{\bar{A}\left(\frac{x'}{r}\right)^2 + \bar{B}\left(\frac{y'}{r}\right)^2 + \bar{C}\left(\frac{z'}{r}\right)^2}{r^4}$$

the scalar components of the perturbing acceleration are given by

$$\ddot{X} = G\left[H\,\frac{x}{r} - \frac{3}{r^5}(\bar{A}m_{11}x' + \bar{B}m_{21}y' + \bar{C}m_{31}z')\right]$$

$$+ GM_e\left[\frac{x_e - x}{\rho_e^3} - \frac{x_e}{R_e^3}\right] + GM_s\left[\frac{x_s - x}{\rho_s^3} - \frac{x_s}{R_s^3}\right] \qquad (8)$$

$$\ddot{Y} = G\left[H\,\frac{y}{r} - \frac{3}{r^5}(\bar{A}m_{12}x' + \bar{B}m_{22}y' + \bar{C}m_{32}z')\right]$$

$$+ GM_e\left[\frac{y_e - y}{\rho_e^3} - \frac{y_e}{R_e^3}\right] + GM_s\left[\frac{y_s - y}{\rho_e^3} - \frac{y_s}{R_e^3}\right] \qquad (9)$$

$$\ddot{Z} = G\left[H\,\frac{z}{r} - \frac{3}{r^5}(\bar{A}m_{13}x' + \bar{B}m_{23}y' + \bar{C}m_{33}z')\right]$$

$$+ GM_e\left[\frac{z_e - z}{\rho_e^3} - \frac{z_e}{R_e^3}\right] + GM_s\left[\frac{z_s - z}{\rho_s^3} - \frac{z_s}{R_s^3}\right] \qquad (10)$$

where

$$\rho_e^2 = (x_e - x)^2 + (y_e - y)^2 + (z_e - z)^2$$

$$R_e^2 = x_e^2 + y_e^2 + z_e^2$$

$$\rho_s^2 = (x_s - x)^2 + (y_s - y)^2 + (z_s - z)^2$$

$$R_s^2 = x_s^2 + y_s^2 + z_s^2 \quad .$$

The inertial coordinates of the satellite are expressed most conveniently as a function of the orbit elements, in the form

$$\begin{aligned} x &= r(\cos u \cos \Omega - \sin u \sin \Omega \cos I) \\ y &= r(\cos u \sin \Omega + \sin u \cos \Omega \cos I) \\ z &= r(\sin u \sin I) \quad . \end{aligned} \tag{11}$$

Finally, employing standard coordinate transformation techniques, it is easy to show that the components of the perturbing acceleration in the radial, circumferential and normal directions are given by

$$\begin{aligned} R = {} & \ddot{X}(\cos u \cos \Omega - \sin u \sin \Omega \cos I) \\ & + \ddot{Y}(\cos u \sin \Omega + \sin u \cos \Omega \cos I) \\ & + \ddot{Z}(\sin u \sin I) \end{aligned} \tag{12}$$

$$\begin{aligned} S = {} & \ddot{X}(- \sin u \cos \Omega - \cos u \sin \Omega \cos I) \\ & + \ddot{Y}(- \sin u \sin \Omega + \cos u \cos \Omega \cos I) \\ & + \ddot{Z}(\cos u \sin I) \end{aligned} \tag{13}$$

$$\begin{aligned} W = {} & \ddot{X}(\sin \Omega \sin I) \\ & + \ddot{Y}(- \cos \Omega \sin I) \\ & + \ddot{Z}(\cos I) \quad . \end{aligned} \tag{14}$$

Equations (1),(2),(3),(4),(8),(9),(10),(11),(12),(13), and (14), were programmed for numerical solution with the

Control Data Corporation 1604 computer at The University of Texas Computation Center.

# III. NUMERICAL COMPUTATION

## A. Computation Procedure

A computer program to integrate the perturbation equations was coded in FORTRAN-63 language[10] for use with the CDC 1604 digital computer. Numerical integration was carried out using a partial double-precision Adams-Moulton method with a fourth-order Runge-Kutta starter.[16] To facilitate integration, all input values are scaled to have the same order of magnitude by dividing quantities which have the length dimension by the factor $10^4$. An initial value of each orbit element and an integration mesh size must be specified by the user. After three starting values are calculated by the Runge-Kutta routine, the Adams-Moulton routine calculates a fifth value based on the previous four values. Integration is continued by the Adams-Moulton procedure, which will also calculate (as an option) the maximum single step error and compare its value with prescribed limits. If limits are exceeded, the mesh size is either doubled or reduced by one-half. For this study a 100 second fixed step size was used, since it was determined that the maximum absolute error never exceeded the limits of $10^{-6}$ and $10^{-11}$.

Each orbit type required approximately 24,000 integration steps. However, only local maximum and minimum values of the orbit elements and corresponding time values are detected and stored by the computer. The intermediate values of the short period variations are dropped, providing a twentyfold saving in computer storage space and some reduction in machine time. A quantitative description of the short period variations for month long study times would be impractical for this analysis. Normalized plots of local maximum and minimum values provide a qualitative description of the envelope of the motion while preserving some quantitative usefulness.

When integration has terminated, local values of each orbit element are scanned for the largest and the smallest value to provide limits for subsequent normalizing. Local values and associated time values are then stored on magnetic tape for later use with a computer plot routine.[23] Normalized values of the orbit elements are plotted against time by the CDC 165 Plotter.

## B. Accuracy Estimation

There are two types of error associated with the numerical computation procedure used in this study. The first type is the familiar and unavoidable computer round-off error. The second type, truncation error, is alway present in any numerical integration scheme. When dealing with highly nonlinear problems, such as this one, it is extremely difficult to make final judgements on how these errors affect the overall accuracy of the results. There are, however, several ways of effectively controlling these errors. The primary requirement for simultaneous control of both types of error is a proper integration mesh size. Too small a mesh size results in more integration steps than are actually necessary, causing excessive error propagation by rounding. Increasing the mesh size reduces round-off error, but if the mesh size is too large, truncation error becomes a problem.

(1) Round-Off Error. Practically all of the computer calculations are carried out using single precision arithmetic which employs 11 decimal digits. The rounding error limit for a single arithmetic operation is $0.5 \times 10^{-12}$. The cumulative effect of this error can be estimated by comparing single precision results with double precision (25 decimal digits) results from the same initial conditions. The results for two 30 orbit computer runs differed at most by $.5 \times 10^{-11}$. This result, however, is based on double precision calculations for the satellite coordinate transformation matrices and for the distrubing acceleration due to the Earth and Sun. This test does indicate no serious error build-up. Use of double precision throughout would, for all practical purposes, eliminate round-off error, but machine time would be increased by a factor of from 20 to 30. A more economical procedure is to use double precision only in arithmetic operations that are most susceptible to round-off error, such as the addition of a small number and a relatively large number. This procedure is used in the Adams-Moulton routine and also in the routine that interpolates for distrubing body coordinates. To help control round-off error in single precision calculations, the terms in the mathematical expressions were arranged according to a set of rules given in Reference 18. In view of these precautions, one might expect

results that are free of this type error through six digits. The final normalized values of the orbit elements would be in error by less than 1%. Precision through five digits would still preserve range accuracy to within ± 100 meters.

(2) Truncation Error. The local truncation error associated with the Adams-Moulton method can be effectively controlled by the error check and mesh size adjustment procedures mentioned previously. For this investigation, however, the highly stable characteristics of the Adams-Moulton method permitted the use of a fixed mesh size, which eliminated the machine time required for error check calculations. The calculated error is an approximation for the true maximum absolute single step error, or the true local truncation error. The single step error was monitored during computer program testing, using a fixed mesh size of 100 seconds and different sets of initial conditions. It was found that the magnitude of the calculated error remained within the limits $2 \times 10^{-9}$ and $8 \times 10^{-11}$. A rough estimate of the upper limit for the accumulative error, based on 24,000 integration steps, assuming no round-off error and error propagation in one direction, would be of the order $10^{-5}$. Since the truncation error can be positive or negative, error build-up to this limit is unlikely. Hence, one would expect at least five digit precision with regard to truncation error. Assuming round-off and truncation error are independent, it would be reasonable to expect overall precision through five digits.

# IV. RESULTS

## A. Specification of Orbit Types

The purpose of this investigation is to analyze the characteristics of circular satellite orbits having near equatorial inclinations. Specific initial conditions are chosen so that results can be compared with the results given in Reference 4. Such a comparison would test computer program validity and, in addition, would provide a basis for evaluating the solar effects.

Eight orbit types are selected for this analysis. Orbits having initial inclinations of 0.5° and 20° are each assigned initial altitudes of 50 miles (P = 1822.20 KM) and 150 miles (P = 1981.35 KM) and are referred to as orbit type 1 through 4 (prograde orbits). Similarly, orbits having initial inclinations of 179.5° and 160° are referred to as orbit type 5 through 8 (retrograde orbits). In all cases initial eccentricity is set at zero (initially circular orbits), and satellite motion starts at the ascending node ($\Omega = 222.113°$), which is a point in the lunar equatorial plane on the side of the Moon opposite the Earth. Hence, the initial value of the argument of pericenter plus the true anomaly is zero ($u = \omega + f = 0$).

Each orbit type is numerically integrated over a period of 27.55 days (i.e., the Moon's anomalistic period).

This time span is equivalent to 341 satellite revolutions for $P = 1822.20$ KM and 301 revolutions for $P = 1981.35$. Results are obtained for the orbit elements P, I, $\Omega$ and e. The element u is not considered because $\omega$ has little significance for circular orbits and because Born[4] found that u has a linear variation, indicating negligible perturbing effects.

## B. Comparison with the Results from Reference 4

A similar investigation carried out by Born is described in the Introduction of this report. Even though there is some difference in mathematical models, the computed times for orbit element local maximum and minimum values are the same, thus allowing direct comparison of element values. Tables 1 and 2 present a comparison of initial and final values of P, I, $\Omega$ and e for 80 revolutions. Unusually close agreement exists for all orbit types. Maximum differences in the final values are as follows: $\Delta P = 8$ meters, $\Delta I = 0.008°$, $\Delta\Omega = 1.134°$ and $\Delta e = 0.0000057$, where $\Delta(\ )$ indicates the difference between the values from the two investigations. Note that the difference in the initial values of $\Omega$ is 0.163°, which accounts for part of the difference in the final values of $\Omega$. It is interesting to note that $\Omega = 222.113°$ is determined by Earth coordinates obtained from JPL tapes, whereas Brown's truncated series expansions lead to the value $\Omega = 222.276°$.

The comparison lends support to the argument that both computer programs are valid, particularly since they were written independently. Some disagreement is expected due to

## TABLE 1

## END POINT DATA COMPARISON FOR 80 SATELLITE REVOLUTIONS--PROGRADE ORBITS

| | | P-KM | | I | | Ω | | e | |
|---|---|---|---|---|---|---|---|---|---|
| Orbit Type | Data Source | Initial | Final | Initial | Final | Initial | Final | Initial | Final |
| 1 | Thesis | 1822.20 | 1822.214 | 0.5° | 0.4685° | 222.113° | 209.739° | 0.0 | 0.0002313 |
| | Born | 1822.20 | 1822.210 | 0.5° | 0.4685° | 222.276° | 210.069° | 0.0 | 0.0002314 |
| 2 | Thesis | 1981.35 | 1980.904 | 0.5° | 0.4690° | 222.113° | 209.800° | 0.0 | 0.0002418 |
| | Born | 1981.35 | 1980.911 | 0.5° | 0.4689° | 222.276° | 210.153° | 0.0 | 0.0002361 |
| 3 | Thesis | 1822.20 | 1822.096 | 20° | 19.618° | 222.113° | 215.769° | 0.0 | 0.0002227 |
| | Born | 1822.20 | 1822.091 | 20° | 19.621° | 222.276° | 215.967° | 0.0 | 0.0002233 |
| 4 | Thesis | 1981.35 | 1980.911 | 20° | 19.7147° | 222.113° | 214.924° | 0.0 | 0.0001774 |
| | Born | 1981.35 | 1980.919 | 20° | 19.7148° | 222.276° | 215.126° | 0.0 | 0.0001784 |

## TABLE 2

### END POINT DATA COMPARISON FOR 80 SATELLITE REVOLUTIONS--RETROGRADE ORBITS

|  |  | P-KM |  | I |  | Ω |  | e |  |
|---|---|---|---|---|---|---|---|---|---|
| Orbit Type | Data Source | Initial | Final | Initial | Final | Initial | Final | Initial | Final |
| 5 | Thesis | 1822.20 | 1822.214 | 179.5° | 179.5183° | 222.113° | 226.816° | 0.0 | 0.000657 |
|  | Born | 1822.20 | 1822.210 | 179.5° | 179.5183° | 222.276° | 227.027 ° | 0.0 | 0.000653 |
| 6 | Thesis | 1981.35 | 1980.907 | 179.5° | 179.5238° | 222.113° | 225.104° | 0.0 | 0.000579 |
|  | Born | 1981.35 | 1980.915 | 179.5° | 179.5237° | 222.276° | 225.374° | 0.0 | 0.000575 |
| 7 | Thesis | 1822.20 | 1822.090 | 160° | 159.573° | 222.113° | 229.401° | 0.0 | 0.000558 |
|  | Born | 1822.20 | 1822.087 | 160° | 159.581° | 222.276° | 229.525° | 0.0 | 0.000555 |
| 8 | Thesis | 1981.35 | 1980.931 | 160° | 159.685° | 222.113° | 226.658° | 0.0 | 0.000499 |
|  | Born | 1981.35 | 1980.939 | 160° | 159.689° | 222.276° | 227.792° | 0.0 | 0.000496 |

dissimilarities in the mathematical models. Born excluded the Sun and considered a fixed Earth-Moon node. Earth ephemerides are generated from different sources and values for the three lunar moments of inertia differed by $7.0 \times 10^{-6}$, $3.0 \times 10^{-6}$ and $5.2 \times 10^{-6}$.

The estimate of solar effects given earlier in this report and the close agreement in the foregoing comparison, indicate that the separate or combined effects of the above mentioned model differences do not appreciably influence the orbit types considered over short periods of time.

## C. Graphical Analysis

The discussion that follows deals with variations of the orbit elements P, I, $\Omega$ and $e$ over a period of 27.55 days. The tabular data are rounded values obtained from computer print-outs and the graphical results are tracings of 32 automatic machine plots. Table 3 (see page 38) presents orbit element boundary values for orbit types 1 through 4 (prograde motion) and Table 4 (see page 39) gives similar data for orbit types 5 through 8 (retrograde motion). The last column of each table lists the maximum variation of each orbit element and is obtained by differencing the tabulated maximum and minimum values.

Graphical presentations of the monthly envelopes of the short period variations are given in Figs. 4 through 19 (pages 46-53). Each individual envelope is obtained by plotting only normalized values of the local maximum and minimum points

## TABLE 3

## BOUNDARY VALUES OF ORBIT ELEMENTS--PROGRADE ORBITS

| Orbit Type | Element | Initial | Final | Maximum | Minimum | Difference |
|---|---|---|---|---|---|---|
| 1 | P-KM | 1822.20 | 1821.971 | 1822.215 | 1821.742 | 0.473 |
| | I | 0.5° | 0.467° | 0.5° | 0.454° | 0.046° |
| | Ω | 222.113° | 176.765° | 222.113° | 176.765° | 45.35° |
| | e | 0.0 | 0.000424 | 0.000815 | 0.0 | 0.000815 |
| 2 | P-KM | 1981.35 | 1981.196 | 1981.367 | 1980.904 | 0.464 |
| | I | 0.5° | 0.456° | 0.5° | 0.446° | 0.054° |
| | Ω | 222.113° | 184.126° | 222.113° | 184.126° | 37.99° |
| | e | 0.0 | 0.000594 | 0.000716 | 0.0 | 0.000716 |
| 3 | P-KM | 1822.20 | 1821.916 | 1822.210 | 1821.650 | 0.560 |
| | I | 20° | 19.800° | 20° | 19.587° | 0.413° |
| | Ω | 222.113° | 189.003° | 222.113° | 189.003° | 33.11° |
| | e | 0.0 | 0.000391 | 0.000757 | 0.0 | 0.000757 |
| 4 | P-KM | 1981.35 | 1981.153 | 1981.360 | 1980.821 | 0.539 |
| | I | 20° | 19.859° | 20° | 19.652° | 0.348° |
| | Ω | 222.113° | 197.066° | 222.113° | 197.066° | 25.05° |
| | e | 0.0 | 0.000539 | 0.000662 | 0.0 | 0.000662 |

## TABLE 4

## BOUNDARY VALUES OF ORBIT ELEMENTS--RETROGRADE ORBITS

| Orbit Type | Element | Initial | Final | Maximum | Minimum | Difference |
|---|---|---|---|---|---|---|
| 5 | P-KM | 1822.20 | 1822.113 | 1822.215 | 1821.745 | 0.470 |
|  | I | 179.5° | 179.570° | 179.570° | 179.5° | 0.069° |
|  | Ω | 222.113° | 250.254° | 250.254° | 222.113° | 28.14° |
|  | e | 0.0 | 0.000448 | 0.000781 | 0.0 | 0.000781 |
| 6 | P-KM | 1981.35 | 1981.059 | 1981.367 | 1980.907 | 0.460 |
|  | I | 179.5° | 179.576° | 179.576° | 179.5° | 0.076° |
|  | Ω | 222.113° | 239.832° | 239.832° | 222.113° | 17.72° |
|  | e | 0.0 | 0.000521 | 0.000675 | 0.0 | 0.000675 |
| 7 | P-KM | 1822.20 | 1822.049 | 1822.206 | 1821.656 | 0.550 |
|  | I | 160° | 160.002° | 160.055° | 159.568° | 0.487° |
|  | Ω | 222.113° | 255.984° | 255.984° | 222.113° | 33.87° |
|  | e | 0.0 | 0.000427 | 0.000745 | 0.0 | 0.000745 |
| 8 | P-KM | 1981.35 | 1981.031 | 1981.356 | 1980.828 | 0.528 |
|  | I | 160° | 160.059° | 160.059° | 159.679° | 0.380° |
|  | Ω | 222.113° | 247.501° | 247.501° | 222.113° | 25.39° |
|  | e | 0.0 | 0.000486 | 0.000644 | 0.0 | 0.000644 |

of the short period oscillations (not shown) against time. Orbit element maximum and minimum values listed on each plot correspond to the ordinate values one and zero, respectively. An element value at any point on a plot may be calculated by adding to the listed minimum value the product of the normalized value and the ordinate range. Note that the very small ranges for P, I, and e appear greatly exaggerated on a normalized scale; however, this method of presenting the data facilitates analysis. The envelopes for Ω and portions of I appear as single lines since the amplitudes of their oscillations are too small to distinguish on the plots. Each graph consists of two separate plots of an orbit element so that comparisons may be made with convenience. Thus graphs for the elements P, Ω and e give a comparison for different inclinations, whereas the graphs for inclination present envelopes for different altitudes. Note that when altitude is the variable, the abscissa must represent time in days only, since each curve is based on a different number of revolutions.

It is important to note that the time span of interest (27.55 days) corresponds to the Moon's period of rotation about its spin axis and, also, to its period of revolution about the Earth. At time zero the projection of the Earth-Moon line on the lunar equatorial plane will coincide with the satellite's line of nodes. The Earth-Moon line will rotate (counterclockwise as viewed from the positive z-axis) through approximately 90° increments every 7 days, such that one complete revolution is described in just under 28 days. The x'-axis (Moon's principal axis of inertia) will always be within 7° of the Earth-Moon line. A knowledge of the position of the Earth and the x'-axis will be useful in interpreting the graphical data.

(1) Semi-Latus Rectum. Curves for the variation of the semi-latus rectum experience a significant change in shape with increasing inclination for prograde orbits and decreasing inclination for retrograde orbits. Envelope boundaries are nearly linear for the equatorial inclinations and evolve into fully developed sinusoidal shapes at inclinations of 20° and 160°. From the graphical data alone there is no way of determining what combination of lunar and terrestrial gravitational effects causes this phenomena. At the time of this writing, the unpublished results from a comparison of numerical data and machine plots for two computer runs provided an explanation. One set of results is based on a Moon and Earth-only mathematical model and the other is based on a Moon-only model. Some of the results are deemed important enough to warrant their inclusion here without presenting a formal graphical justification. Each orbit had an initial inclination of 170° and radius of 1822.20 KM. A comparison of the machine plots of the monthly envelopes for the semi-latus rectum revealed that the shape of the envelope boundaries was practically the same in each case, and that all points of the lower boundary of the Moon-only envelope were about 40 meters (one-tenth increment on the normalized scale) above the Moon and Earth-only lower boundary. This evidence tends to support the contention that lunar effects are much more important than terrestrial effects with

respect to the shape and amplitude of the envelope for the short period oscillations of the semi-latus rectum. By comparing Fig. 4 with Fig. 5 and Fig. 12 with Fig. 13, it is evident that envelope shape is practically independent of altitude for a given inclination. Note that for a given altitude and inclination, the amplitude of oscillations does not depend on the direction of satellite motion. Note, also, that the envelopes for prograde motion (orbit types 1-4) have a 12 day period as opposed to a 14 day period for retrograde motion (orbit types 5-8). In view of what has been said about the motion of the Earth-Moon line and the x'-axis, bi-monthly periods would be expected. The two day difference in the periods can be attributed to the effects of a large nodal regression rate for prograde motion and a nodal progression rate of comparable magnitude for retrograde orbits.

(2) Inclination. The results for the inclination are presented in Figs. 6, 7, 14 and 15. It can be seen that the amplitudes of the short period oscillations are quite small for all orbit types. Note that all envelopes appear to have a secular trend. This is most apparent for orbit types 5 and 6. The test comparison, mentioned previously, revealed that secular trends were not present in the Moon-only plot for inclination. Successive minimum points on the envelope for inclination in the Moon and Earth case differed by 0.2 on the normalized scale. Apparently the Earth alone causes this secular or long-term variation. When the Earth exerts a force normal to the orbit plane, the effect is transmitted to $\dot{I}$ by the force

term (W) in Eq. (4). The direction in which this perturbing force acts determines the direction of the secular variation. Note that an increase in altitude causes an increase in the range of variation of inclination for orbit types 1, 2, 5 and 6 and the range decreases with altitude for orbit types 3, 4, 7 and 8. This rather striking reversal provides a clue for estimating the relative importance of Earth and Moon effects on inclination. Since the range of $I$ is relatively small for the near equatorial inclinations, the effects of small terrestrial forces become apparent when the change in altitude is toward the Earth. On the other hand, the relatively large range of $I$ at inclinations of 20° and 160° indicate that lunar force effects have become much more dominant, causing the range of $I$ to decrease with increasing altitude. In this case the effect of a small increase in the terrestrial force is not noticeable. Born's results show that the critical inclination for reversal must be less than 10°. Finally, note that the periods of the long-term variations are, once again, 12 and 14 days.

(3) Longitude of Ascending Node. The envelopes for the short period oscillations of $\Omega$ are shown as single lines for reasons discussed previously. Actually, the width of these lines is a reasonable estimate for the width of the envelopes (Figs. 8, 9, 16 and 17). The gaps appearing in curves for $\Omega$ denote the absence of local critical points, meaning that, here, the element varies monatonically. A comparison of the results obtained from the two computer runs showed that the change in $\Omega$

due to Earth effects was 0.63°, which is small compared to the total change of 34.9°. Apparently the Moon's triaxiality is the dominant factor with regard to the variation of the node for near-lunar satellites. Figures 8 and 9 show that the node regresses for prograde orbits and Figs. 16 and 17 show a progressing node for retrograde orbits. This is to be expected since the sign of $W$ (the perturbing force normal to the orbit plane) in the equation for $\dot{\Omega}$ is negative when prograde motion exists and positive for retrograde motion. Note that the range of variation of $\Omega$ increases with decreasing altitude for a given inclination. This is so because the Moon appears to be the dominant factor in this case. Although almost all of the curves for $\Omega$ are nearly linear, it is still possible to determine the periods of the long-term variations. They are not significantly different from those noted for $P$ and $I$. The gaps tend to appear when the $x'$-axis is either parallel or perpendicular to the orbit's line of nodes.

(4) Eccentricity. The graphical results for the eccentricity indicate that this element experiences no significant change when altitude, inclination and the direction of satellite motion is changed (Figs. 10, 11, 18 and 19). The maximum value of $e$ increases slightly with decreasing altitude. A similar increase occurs when the direction of satellite motion is reversed (retrograde to prograde). The results of the two computer runs, testing for the separate effects of the Earth and Moon, indicate that subharmonics occurring near

the 7 and 21 day points are caused by the Moon's noncentral force field. Adding in the Earth effects simply causes a slight contraction of the envelopes at these points.

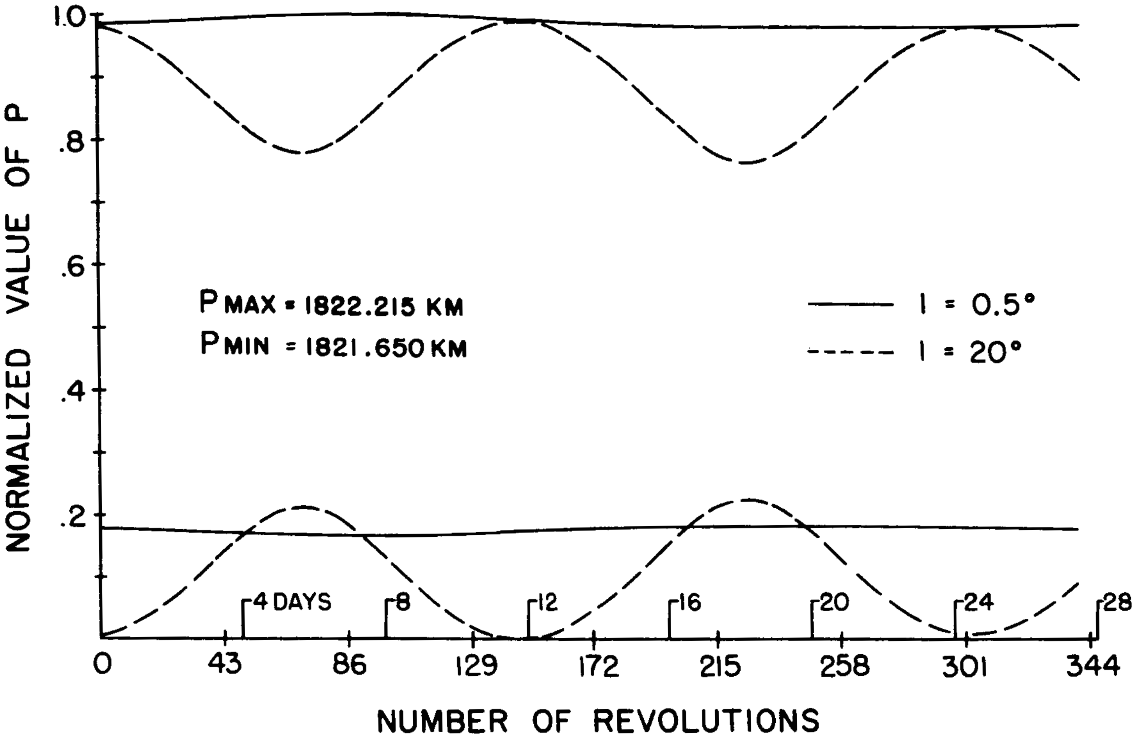

FIGURE 4. SEMI-LATUS RECTUM FOR ORBIT TYPES 1 AND 3.

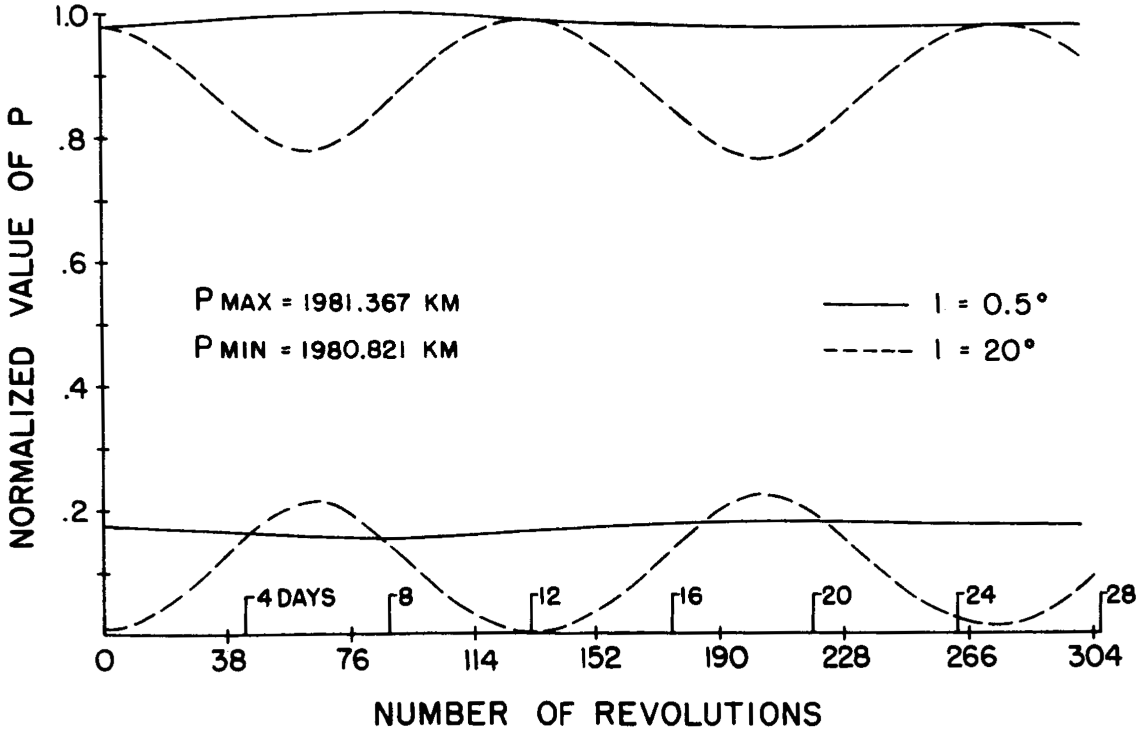

FIGURE 5. SEMI-LATUS RECTUM FOR ORBIT TYPES 2 AND 4.

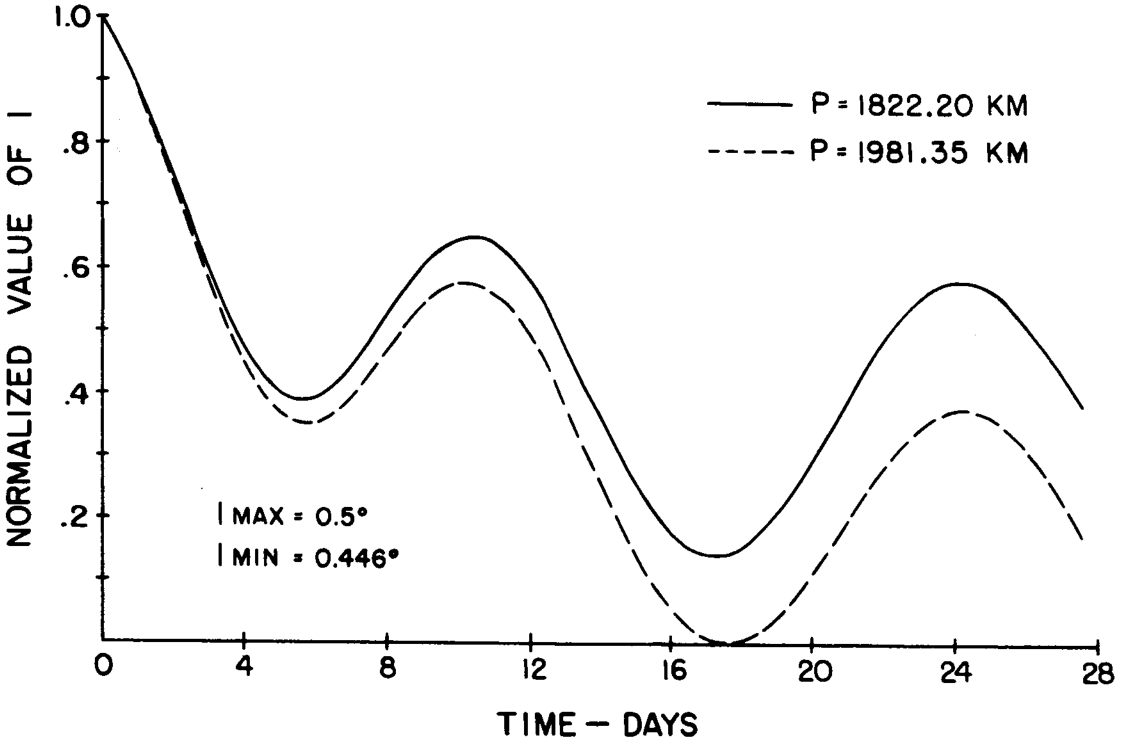

FIGURE 6. INCLINATION FOR ORBIT TYPES 1 AND 2.

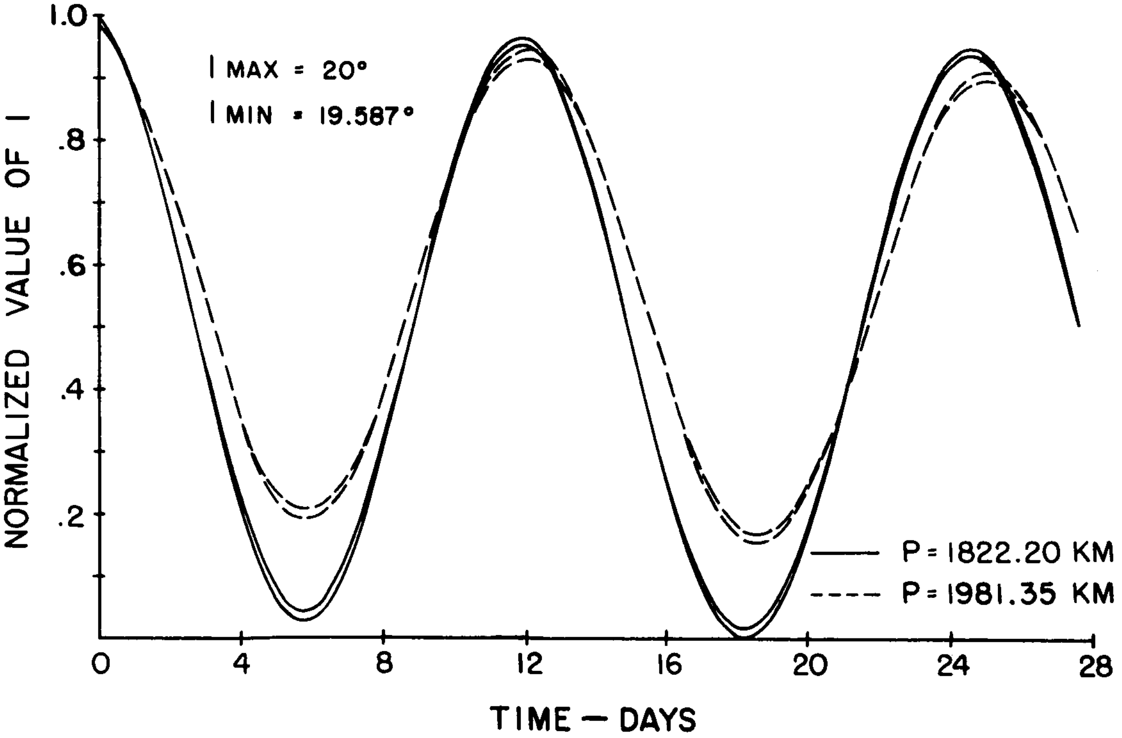

FIGURE 7. INCLINATION FOR ORBIT TYPES 3 AND 4.

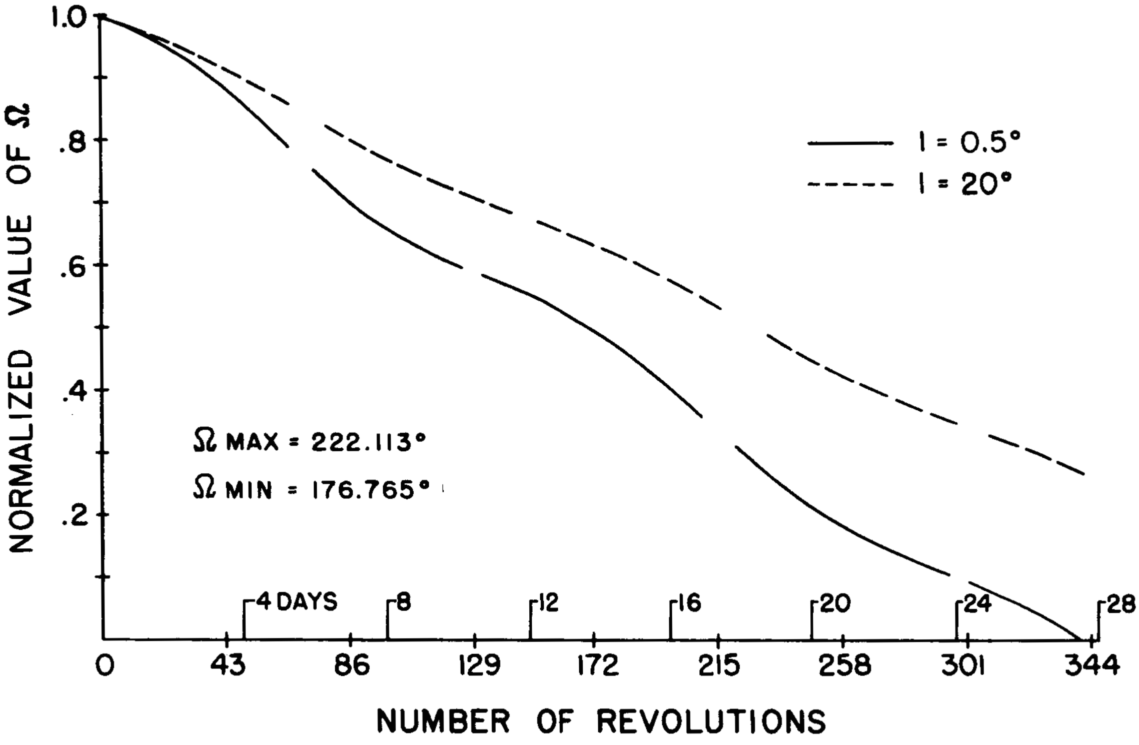

FIGURE 8. ARGUMENT OF NODE FOR ORBIT TYPES 1 AND 3, P=1822.20 KM.

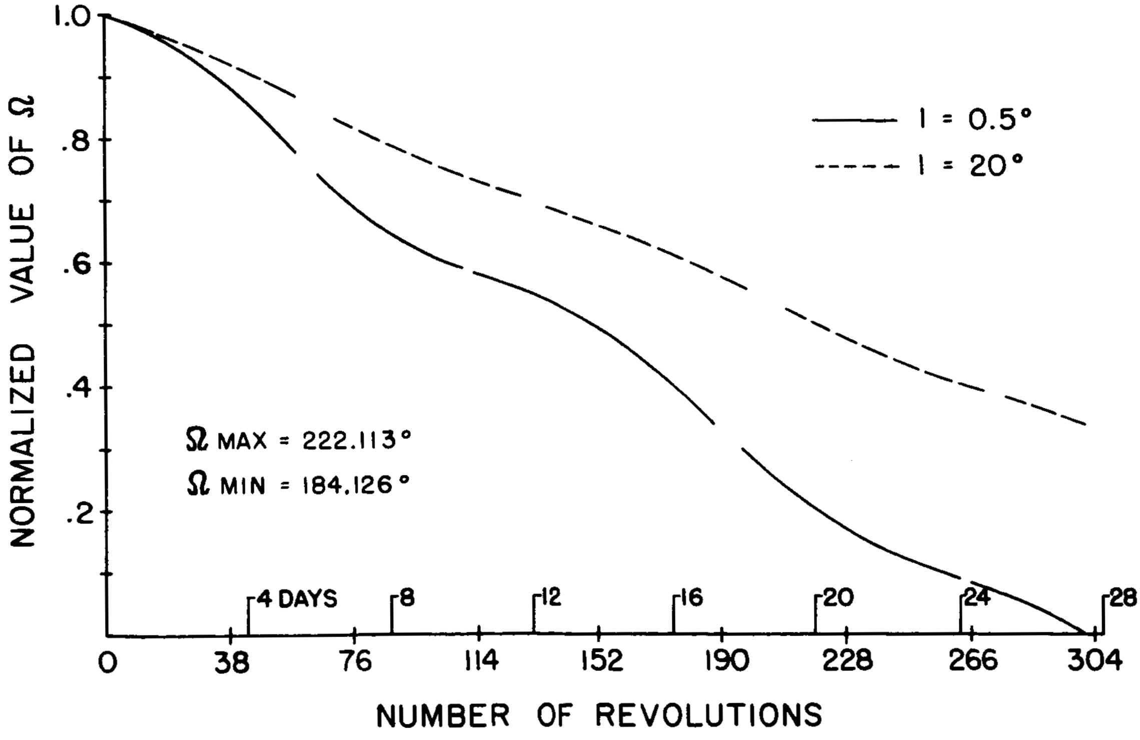

FIGURE 9. ARGUMENT OF NODE FOR ORBIT TYPES 2 AND 4, P=1981.35 KM.

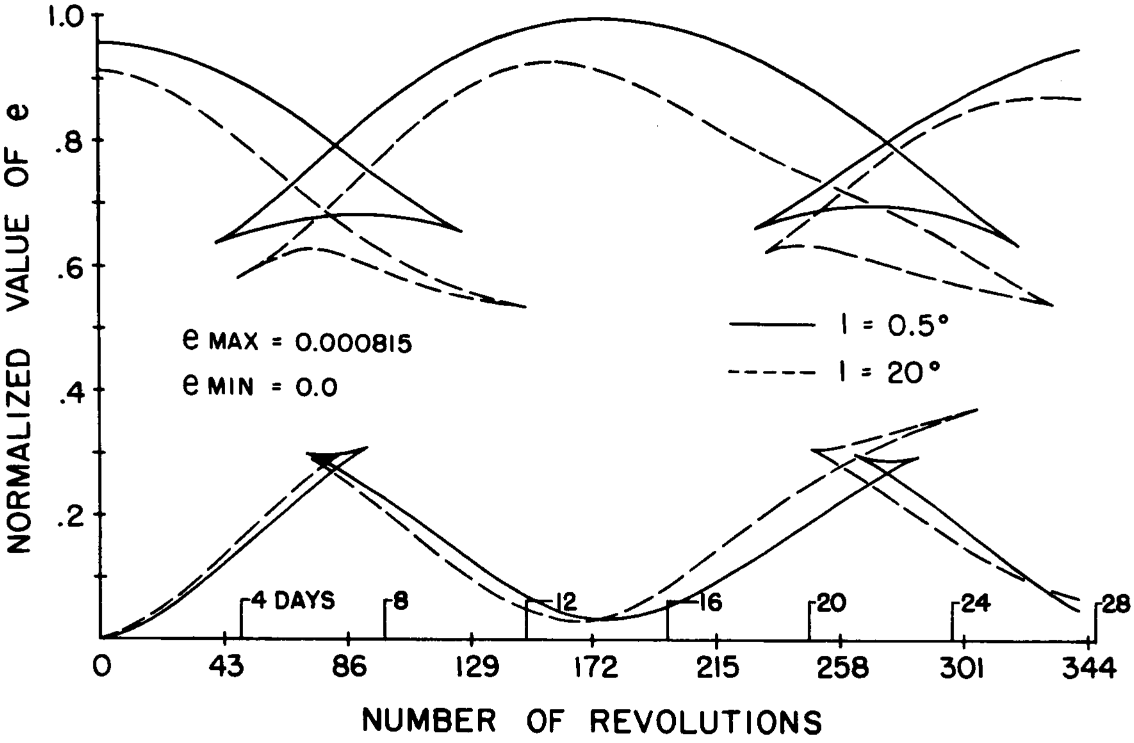

FIGURE 10. ECCENTRICITY FOR ORBIT TYPES 1 AND 3, P=1822.20 KM.

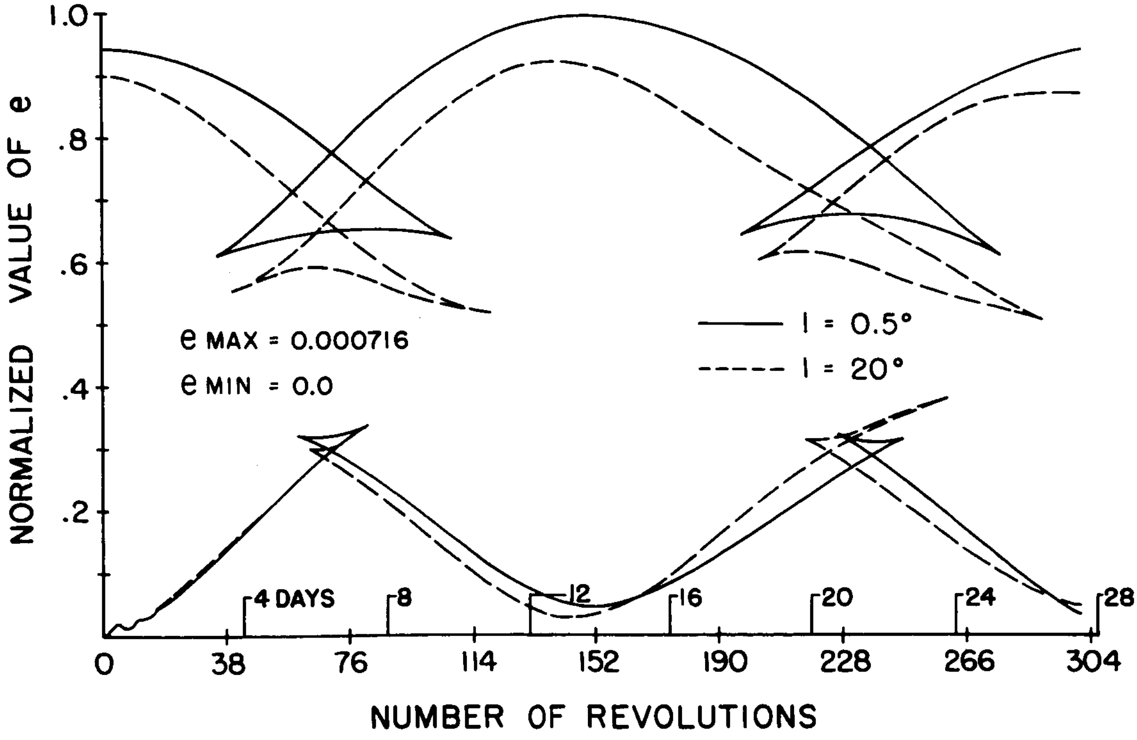

FIGURE 11. ECCENTRICITY FOR ORBIT TYPES 2 AND 4, P=1981.35 KM.

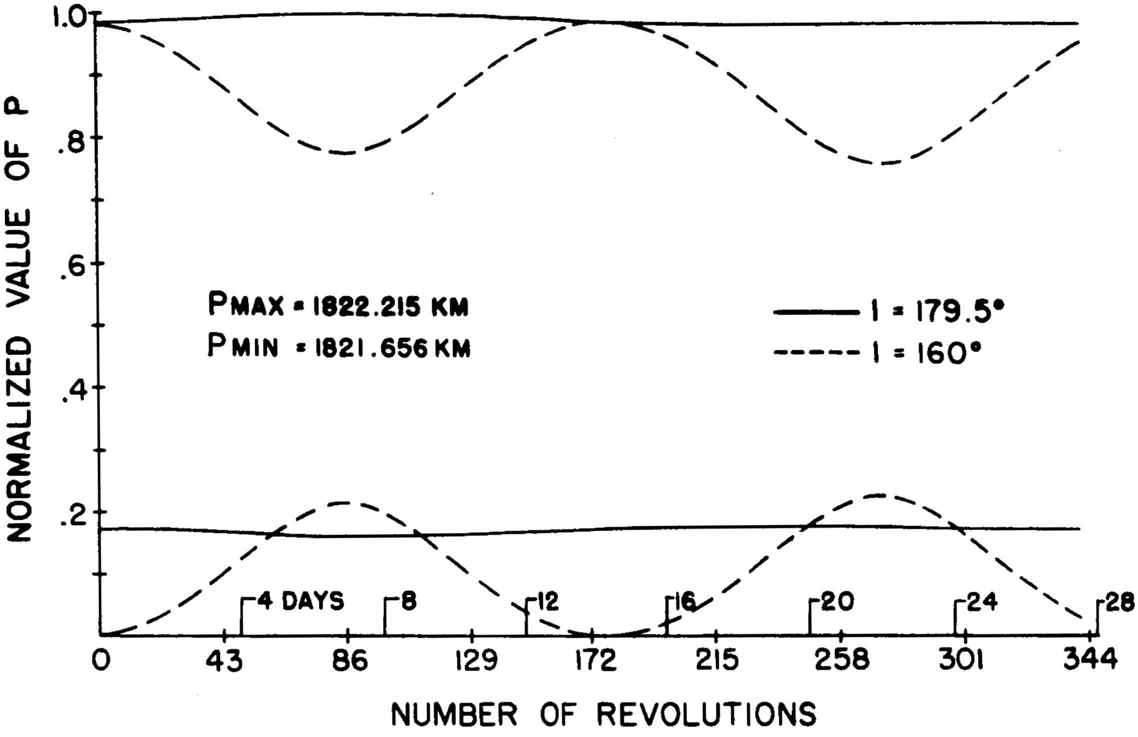

FIGURE 12. SEMI-LATUS RECTUM FOR ORBIT TYPES 5 AND 7.

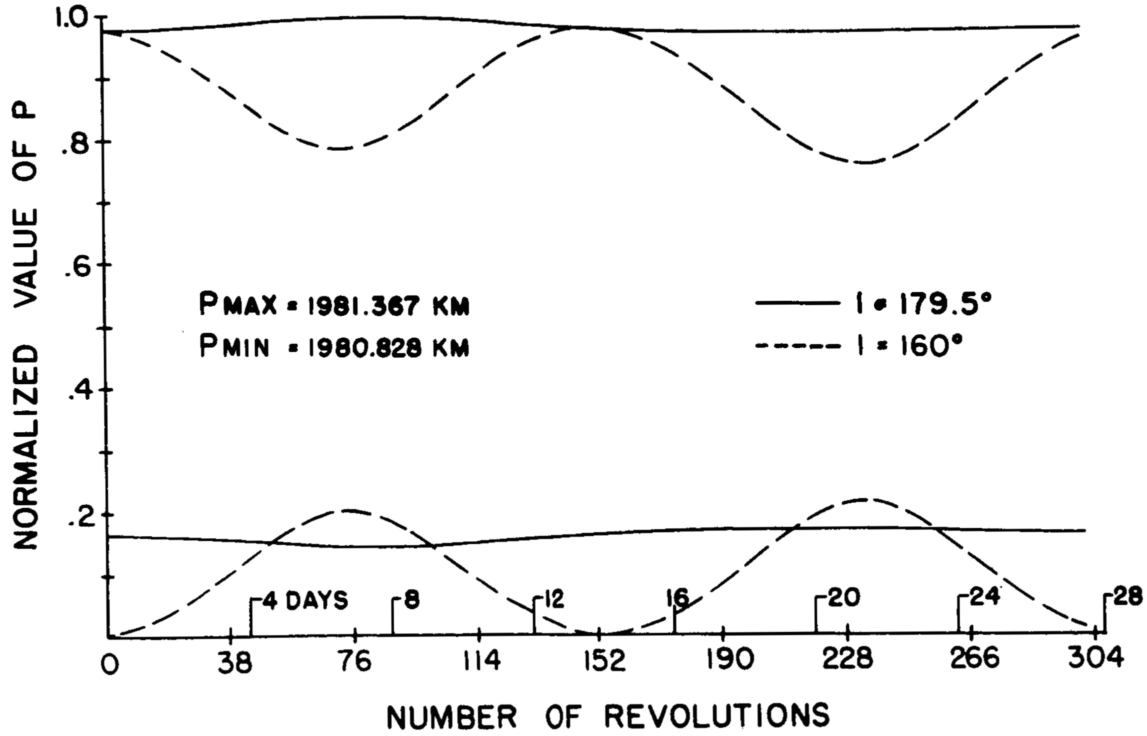

FIGURE 13. SEMI-LATUS RECTUM FOR ORBIT TYPES 6 AND 8.

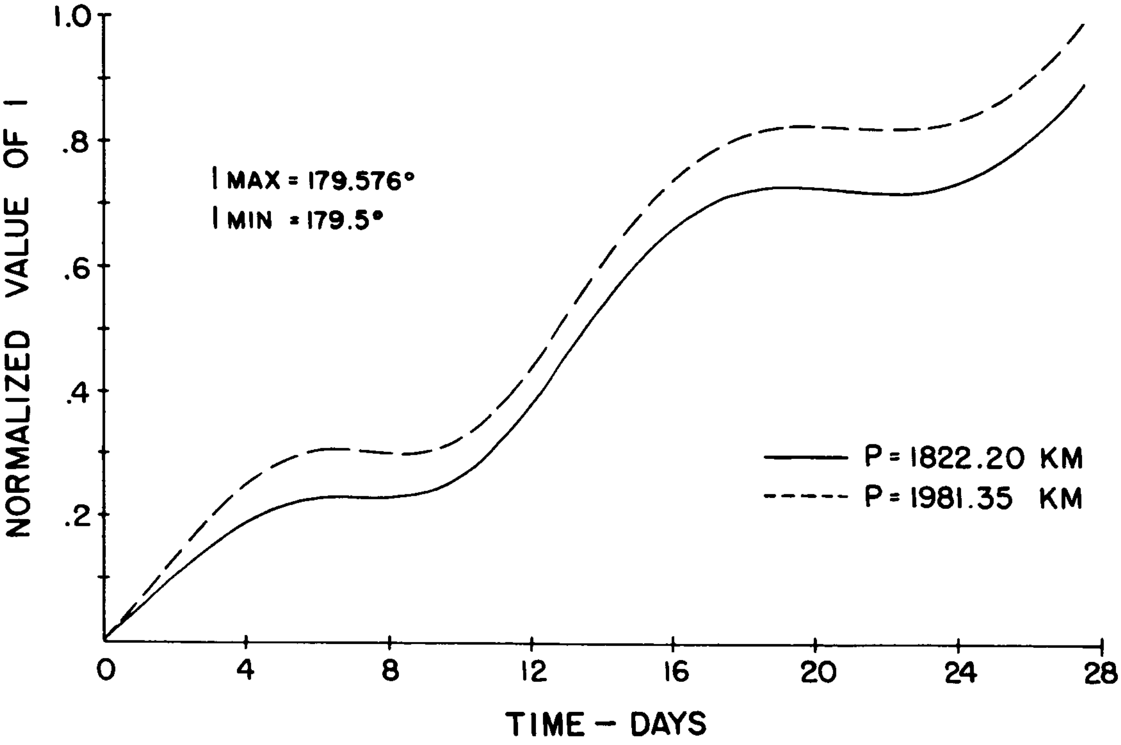

FIGURE 14. INCLINATION FOR ORBIT TYPES 5 AND 6.

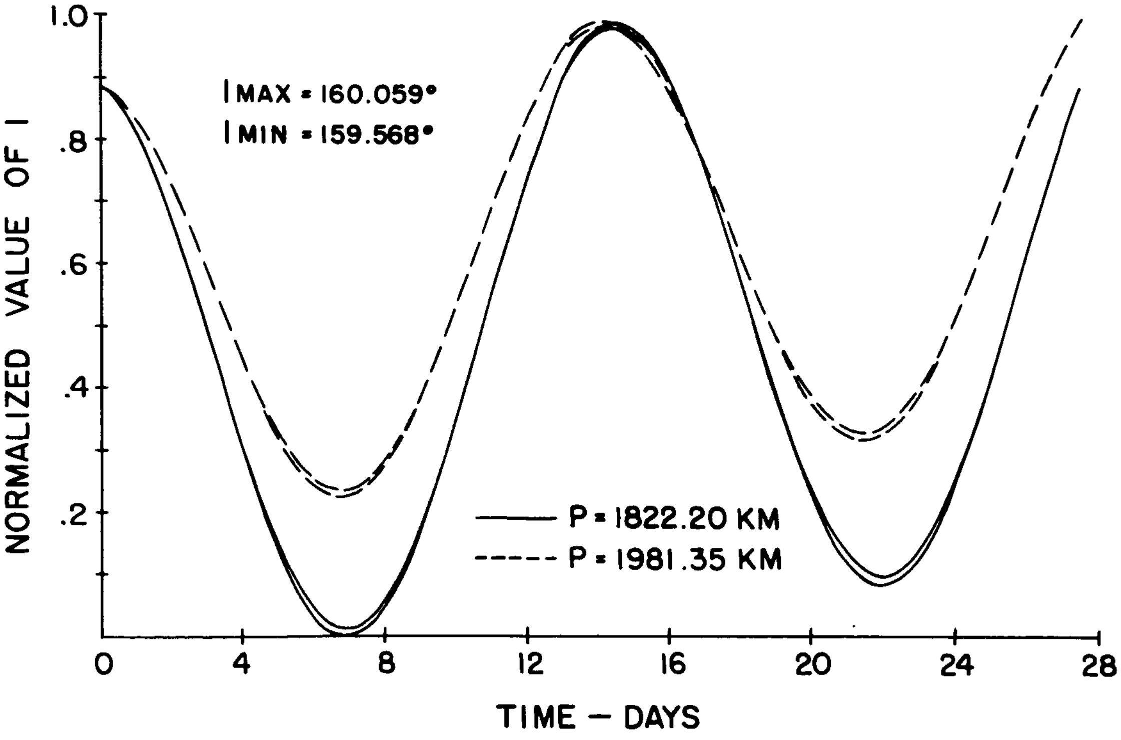

FIGURE 15. INCLINATION FOR ORBIT TYPES 7 AND 8.

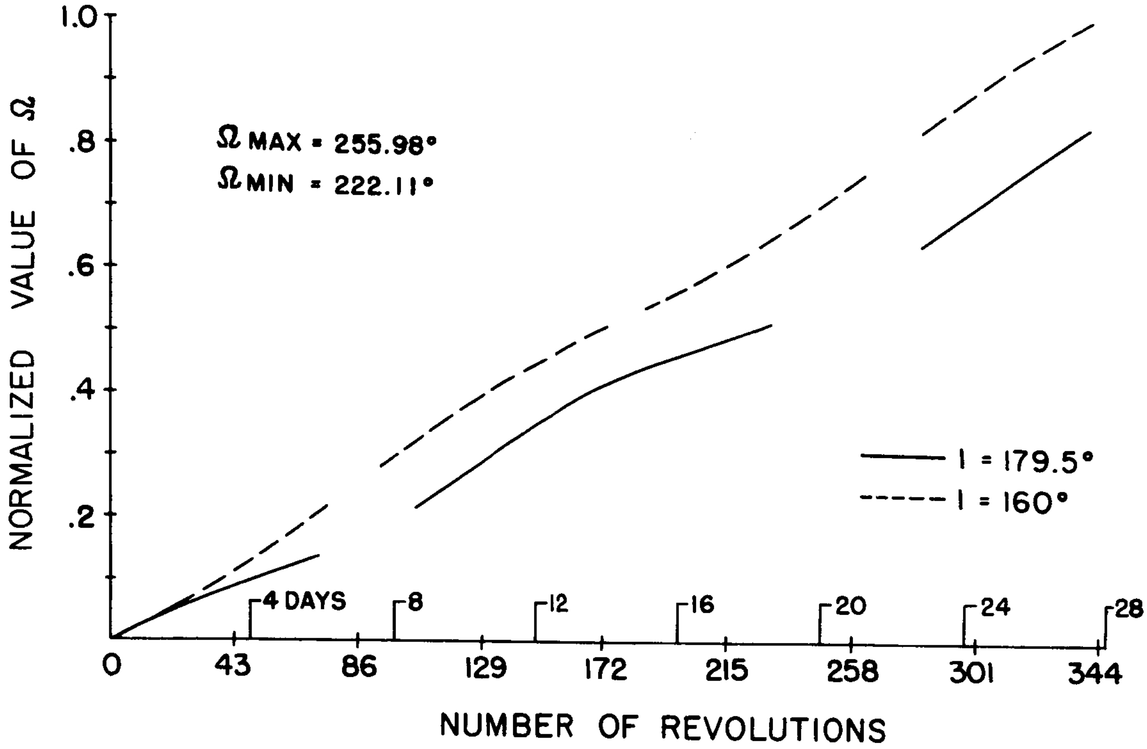

FIGURE 16. ARGUMENT OF NODE FOR ORBIT TYPES 5 AND 7, P=1822.20 KM.

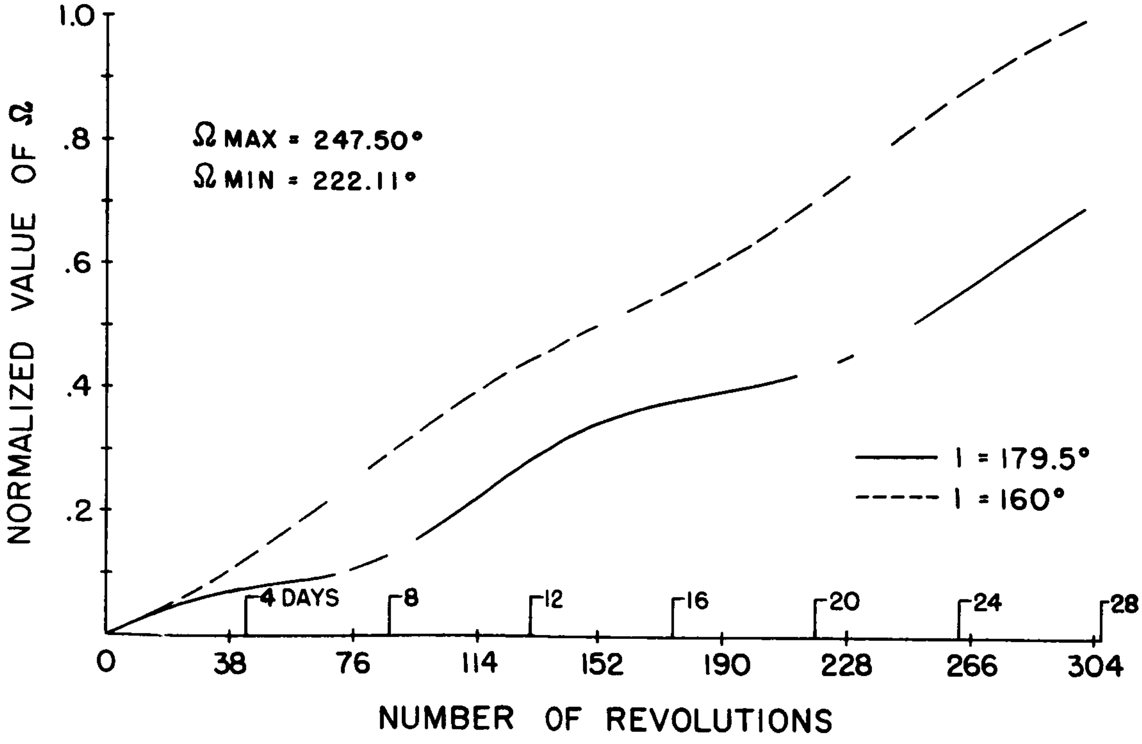

FIGURE 17. ARGUMENT OF NODE FOR ORBIT TYPES 6 AND 8, P=1981.35 KM.

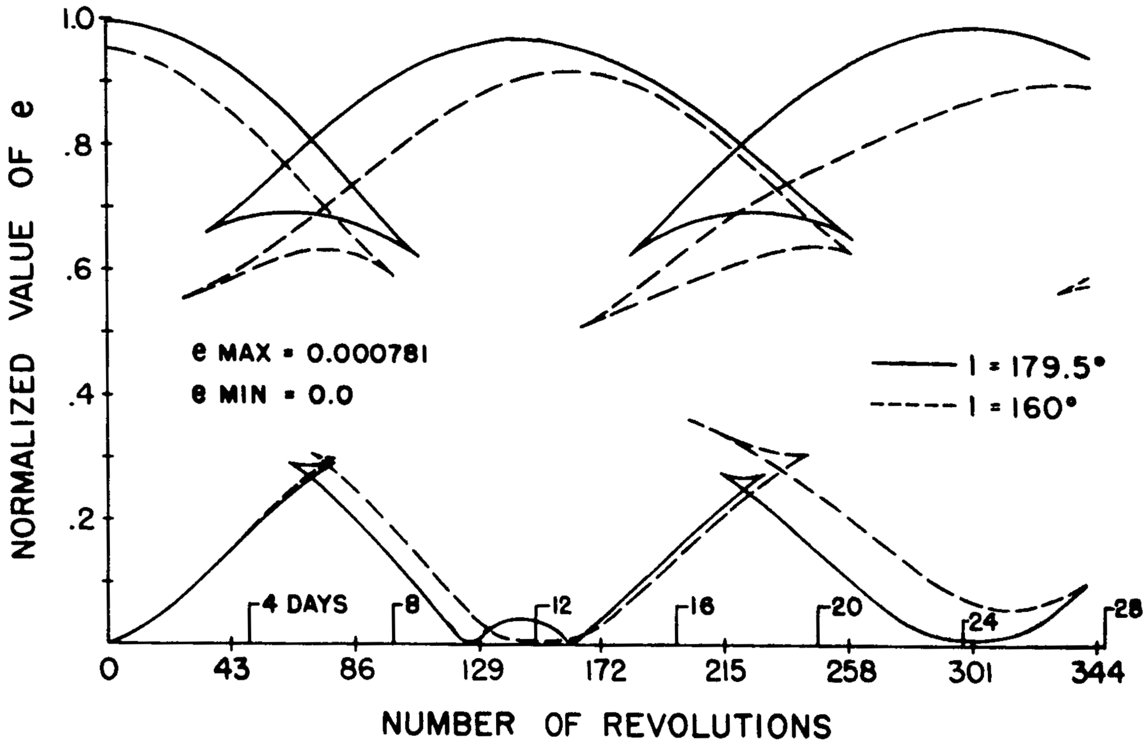

FIGURE 18. ECCENTRICITY FOR ORBIT TYPES 5 AND 7, P=1822.20 KM.

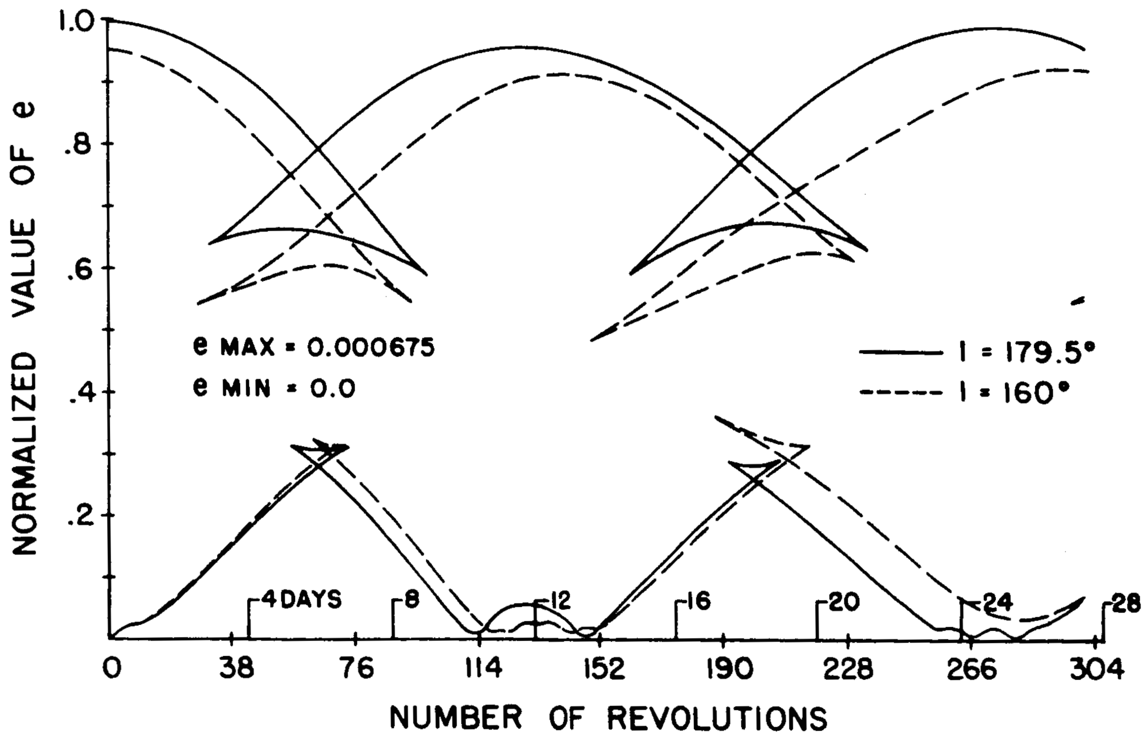

FIGURE 19. ECCENTRICITY FOR ORBIT TYPES 6 AND 8, P=1981.35 KM.

# V. CONCLUSIONS AND RECOMMENDATIONS

A computer program was written to be used with the CDC 1604 digital computer for integration of a set of first-order nonlinear differential equations which define the time rates of change of the satellite orbit elements. The program incorporates an Adams-Moulton numerical integration method with a Runge-Kutta starter. Machine plots for the variation of the orbit elements with respect to time were used to analyze the characteristics of near-circular lunar satellite orbits over a period of approximately 28 days.

The tabular and graphical results for eight orbit types have led to the following conclusions:

(1) All orbit types exhibit highly stable characteristics over an interval of 27.55 days. The appearance of secular trends in the envelopes of the short-period variations of inclination should not be interpreted as an indicator of future instability, since the trends shown may be portions of long-term periodic variations.

(2) The envelopes of the short-term oscillations of values of the orbit elements $P$, $I$, $\Omega$ and $e$ have periods of 12 days for prograde orbits and 14 days for retrograde orbits.

(3) The shape of the envelopes for the semi-latus rectum is sensitive to changes in inclination and relatively insensitive to changes in altitude.

(4) The variational range of the envelopes for the inclination increases with altitude at initial inclinations of 0.5° and 179.5° and decreases with altitude at inclinations of 20° and 160°. Hence, it appears that for short-term motion, the Earth effects are relatively unimportant with respect to significant perturbations in inclination.

(5) The amplitude of the long-term oscillations of the inclination increases significantly when the orbit plane becomes more inclined to the lunar equatorial plane. The principal cause of the phenomena appears to be the component of the Moon's noncentral gravitational force normal to the satellite orbit plane.

(6) The line of nodes regresses for prograde orbits and progresses for retrograde orbits. The secular rate of change of $\Omega$ decreases with altitude for a given inclination and decreases with increasing inclination for a given altitude.

(7) The amplitude of short-period oscillations of the eccentricity are noticeably insensitive to changes in either altitude or inclination.

(8) The manner and extent to which the Earth influences the variation of $P$, $\Omega$, and $e$ cannot be determined from the graphical data given in this report.

Undoubtedly, a more extensive investigation, by machine computation, of certain areas of this problem would lead to more specific interpretations of the graphical data, and would provide a means of improving the method of solution. Some areas of interest are:

(1) Comparing machine plots based on mathematical models that include individual and collective effects of the Moon, Earth, Sun and variable Earth-Moon node would establish criteria for simplifying the problem commensurate with desired accuracy limits.

(2) Computer test runs, exploiting the double precision feature, could establish definite limits for truncation and round-off error.

(3) A significant reduction in machine time can be realized by generating specialized ephemeris tapes containing single precision disturbing body coordinates with a time increment to match the value of a fixed integration mesh size.

(4) For near-lunar orbits, determination of the importance of the fourth-order term of the lunar gravitational potential function would provide a check on the validity of results based on the second-order term only.

# REFERENCES

1. The American Ephemeris and Nautical Almanac, United States Government Printing Office, Washington, D. C., 1966.

2. Battin, R. H., Astronomical Guidance, McGraw-Hill Book Company, New York, 1964.

3. Blanco, V. M., and S. W. McCuskey, Basic Physics of the Solar System, Addison-Wesley Publishing Co., Inc., Reading, Mass., 1961.

4. Born, G. H., "Characteristics of Apollo-Type Lunar Orbits," M.S. Thesis, The University of Texas, January, 1965.

5. Brouwer, D., and G. M. Clemence, Methods of Celestial Mechanics, Academic Press, Inc., New York, 1961.

6. Brumberg, V. A., S. N. Kirpichnikov and G. A. Chebrotarev, "Orbits of Artificial Moon Satellites," Soviet Astronomy, July-August, 1961, pp. 95-105.

7. Clark, J. R., "A Solar System Ephemeris for 1950 to 2000," M.S. Thesis, The University of Texas, January, 1965.

8. Clarke, V. C., Jr., "Constants and Related Data for Use in Trajectory Calculations," JPL Technical Report No. 32-604, March 6, 1964

9. Danby, J. M. A., Fundamentals of Celestial Mechanics, MacMillan Co., New York, 1962.

10. FORTRAN 63/Reference Manual, Control Data Corporation, 8100 34th Avenue South, Minneapolis 20, Minnesota, June, 1964, Revision A.

11. Goddard, D. S., "The Motion of a Near Lunar Satellite," M.S. Thesis, The University of Texas, August, 1963.

12. Holdridge, D. B., "Space Trajectories Program for the IBM 7090 Computer," JPL Technical Report No. 32-223, March 2, 1962.

13. Kalensher, B. E., "Selenographic Coordinates," JPL Technical Report No. 32-41, February 24, 1961.

14. Kaula, W. M., The Investigation of the Gravitational Fields of the Moon and Planets with Artificial Satellites, Vol. 5 of Advances in Space Science and Technology, Academic Press, Inc., 1963.

15. Lass, H., and C. Solloway, "Motion of a Satellite of the Moon," ARS Jr., February, 1961, pp. 220-221.

16. Lastman, G. J., "Solution of n Simultaneous First-Order Differential Equations by the Adams-Moulton Method Using a Runge-Kutta Starter and Partial Double-Precision Arithmetic," UTD2-04-047 (D2 UTEX RKAMSUB), The University of Texas Computation Center, March, 1964.

17. Lorell, J., "Characteristics of Lunar Satellite Orbits," Jet Propulsion Laboratories, Technical Memorandum 312-164, February, 1962.

18. McCraken, D. D., and W. S. Dorn, Numerical Methods and FORTRAN Programming, John Wiley and Sons, Inc., New York, 1964.

19. McCuskey, S. W., Introduction to Celestial Mechanics, Addison-Wesley Publishing Co., Inc., Reading, Mass., 1963.

20. Moulton, F. R., An Introduction to Celestial Mechanics, MacMillan Co., New York, 1964.

21. Nelson, W. C., and E. E. Loft, Space Mechanics, Prentice-Hall, Inc., Englewood Cliffs, New Jersey, 1962.

22. Peabody, P. R., Scott, J. F. and Orozco, E. G., "JPL Ephemeris Tapes E9510, E9511, and E9512," JPL Technical Memorandum No. 33-167, March 2, 1964.

23. Singleton, D., "FORTRAN-63 Plot Routine," UTQ4-01-064 (Q4 UTEX PLOT63), The University of Texas Computation Center, February, 1965.

24. Tolson, R. H., "The Motion of a Lunar Satellite Under the Influence of the Moon's Noncentral Force Field," M.S. Thesis, Virginia Polytechnic Inst., April, 1963.

25. Wells, W. R., "ANalytical Lifetime Studies of a Close-Lunar Satellite," NASA Technical Note D-2805, Langley Research Center, Va., May, 1965.

# VITA

David Hawkins, the son of Mary and Allen Hawkins, was born in East Orange, New Jersey, on January 7, 1931. He graduated from Columbia High School, Maplewood, New Jersey, in 1949, and received the Bachelor of Science Degree in Mathematics from Trinity College, Hartford, Connecticut, in 1954. Through the R. O. T. C. Program at Trinity, he was commissioned a Second Lieutenant in the United States Air Force. Following three years of training in piloting, navigation and bombing, he spent five years in the Strategic Air Command as a navigator-bombadier on a combat-ready B-52 bomber crew. In 1960 he married the former Rosa Louise Andrews of Montgomery, Alabama, while attending the Air Force Squadron Officers School at Maxwell AFB. He enrolled in The University of Texas in 1962, under The Air Force Institute of Technology Program and received the Bachelor of Science Degree in Aero-Space Engineering in 1965. He now holds the rank of Captain USAF.

Permanent address: 350 Hartford Road
South Orange, New Jersey

This thesis was typed by Mrs. Patricia J. McIlvain.